Supporting Information

Solution-Processed Spin Organic Light-Emitting Diodes Based on Antisolvent-Treated 2D Chiral Perovskites with Strong Spin-Dependent Carrier Transport

Lan-Sheng Yang*, Chun-Yao Huang, Chin-An Hsu, Sih-Tong Lin, Yun-Shan Hsu,Chia-Hsiang Chuang, Pei-Hsuan Lo, Yu-Chiang Chao*
Department of Physics
National Taiwan Normal University
Taipei 11677, Taiwan, R.O.C.
E-mail: s10365love@gmail.com ycchao@ntnu.edu.tw

Key words: Chiral perovskites, circular dichroism, circularly polarized photoluminescence, Circularly polarized electroluminescence, Spin organic light-emitting diodes

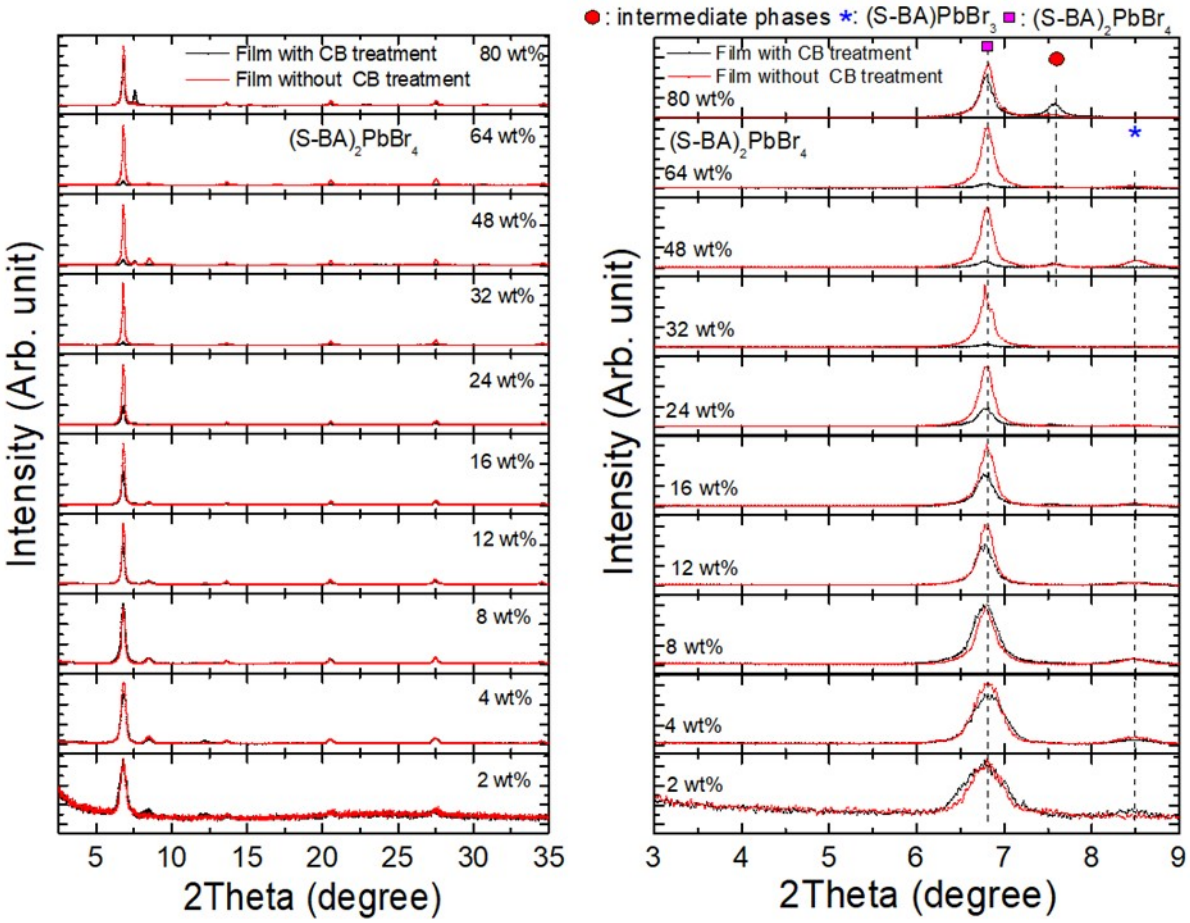

Figure S1: The XRD of the CB-treated and untreated $(S\text{-}BA)_2PbBr_4$ films with different concentration chiral perovskite precursors.

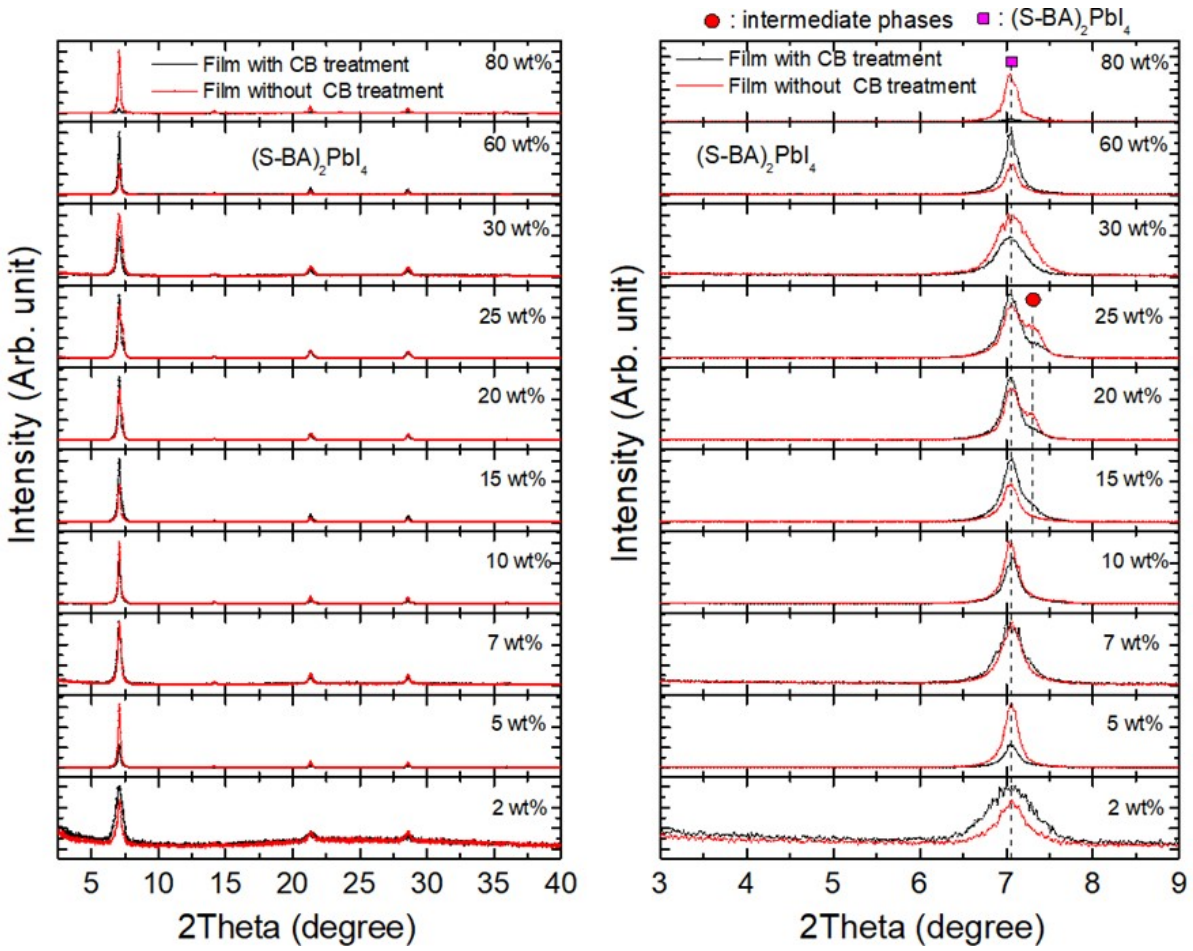

Figure S2: The XRD of the CB-treated and untreated $(S\text{-}BA)_2PbI_4$ films with different concentration chiral perovskite precursors.

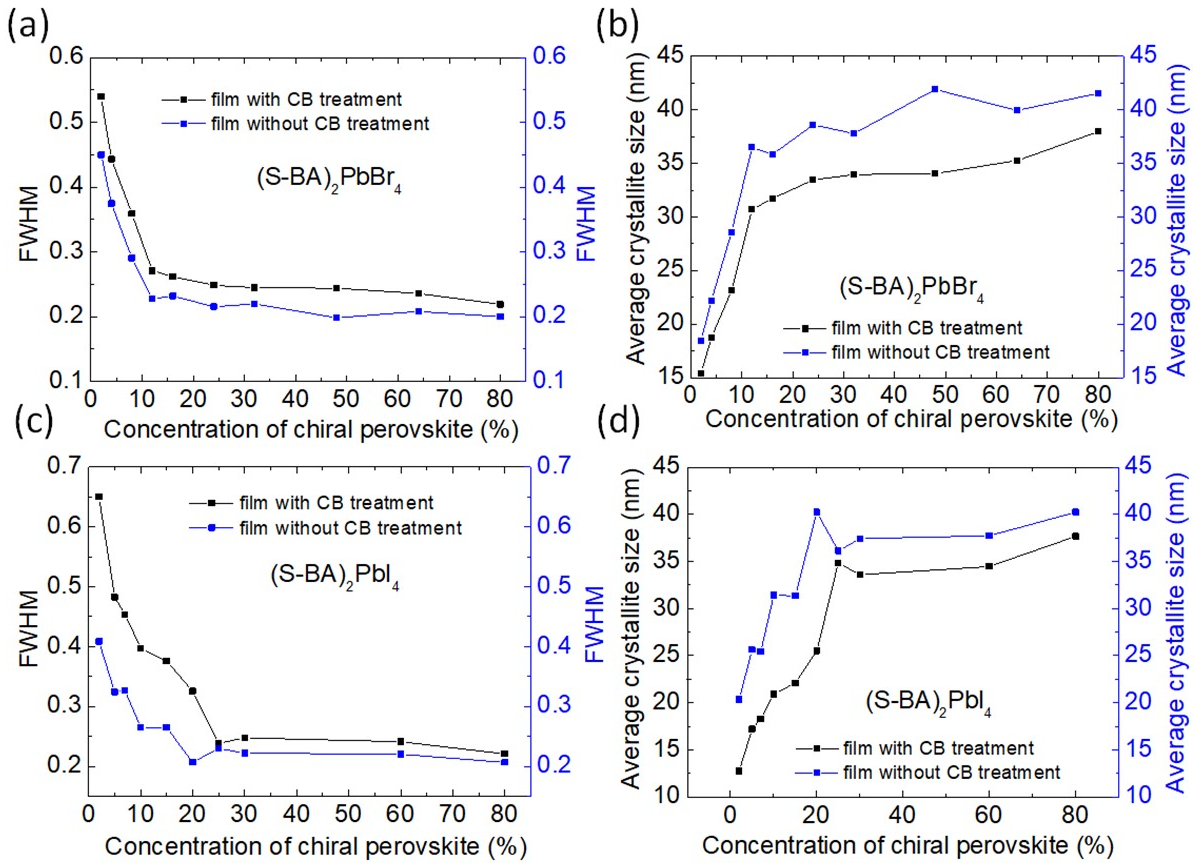

Figure S3: The (a,c) FWHM and (b,d) average crystallite size of the CB-treated and untreated $(S\text{-}BA)_2PbBr_4$ and $(S\text{-}BA)_2PbI_4$films with different concentrations of chiral perovskite.

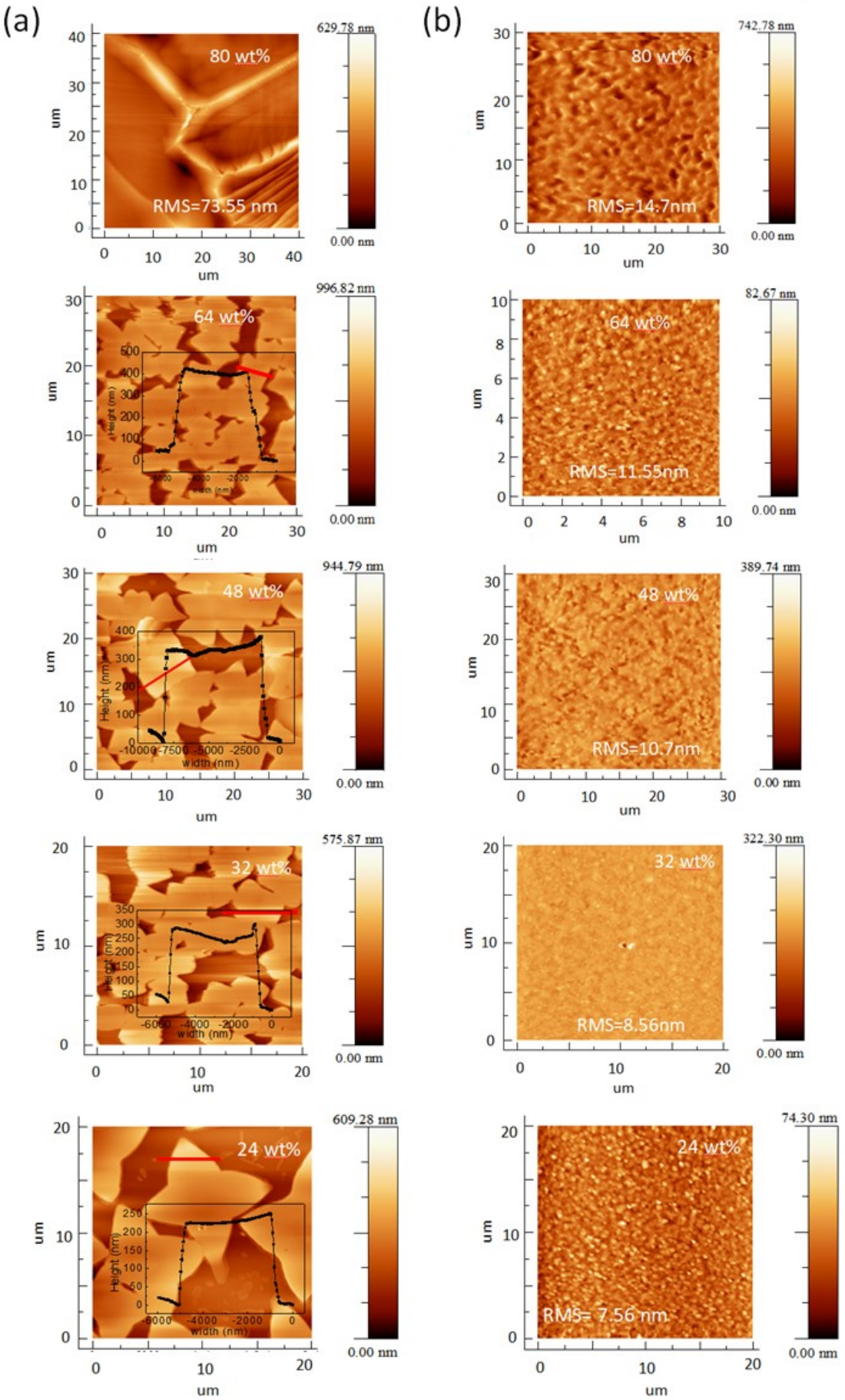

Figure S4: The AFM image of $(S\text{-}BA)_2PbBr_4$ films(a) without and (b) with CB treatment for different concentration of chiral perovskite

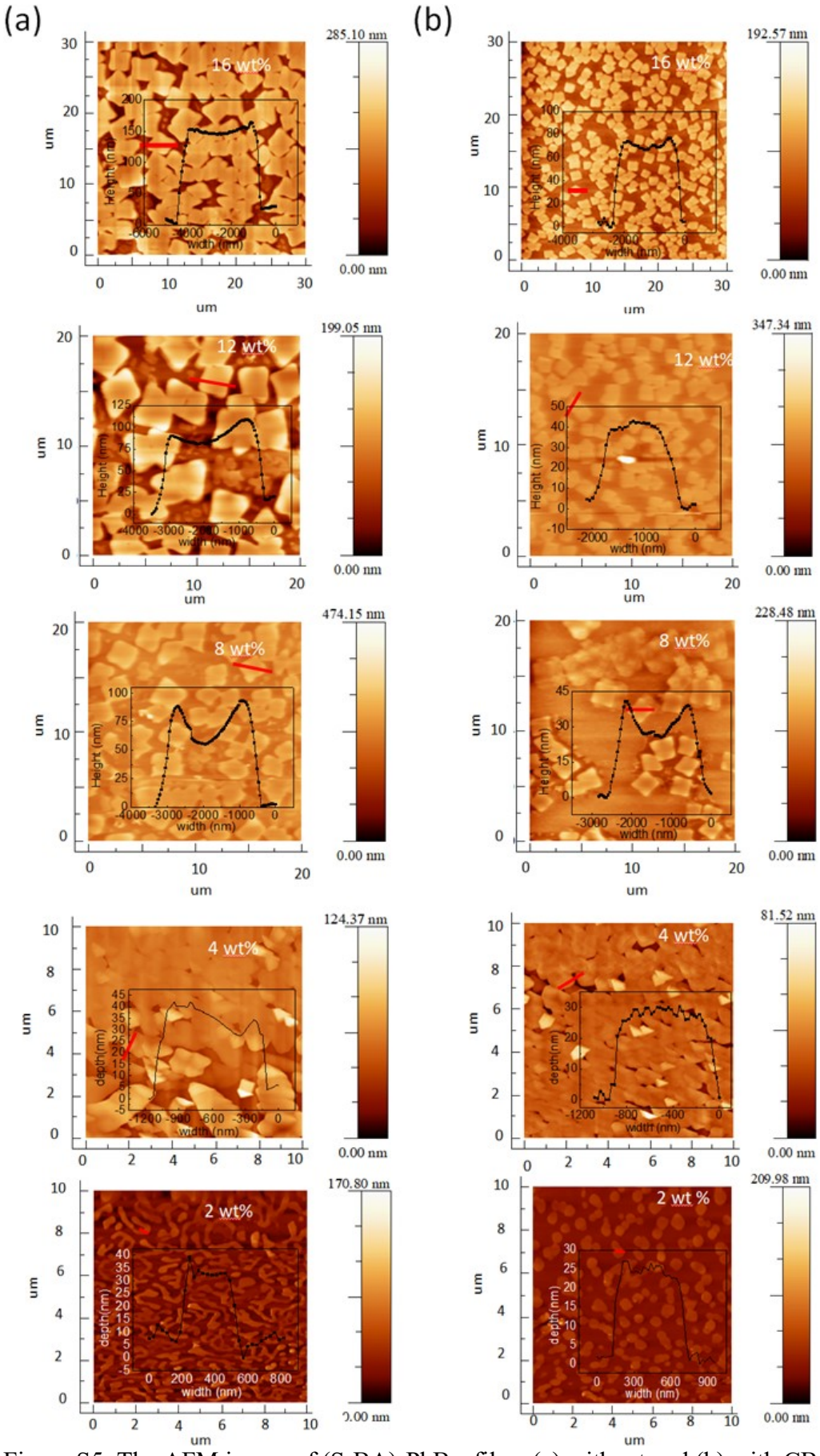

Figure S5: The AFM image of $(S\text{-}BA)_2PbBr_4$ films (a) without and (b) with CB treatment for different concentration of chiral perovskite

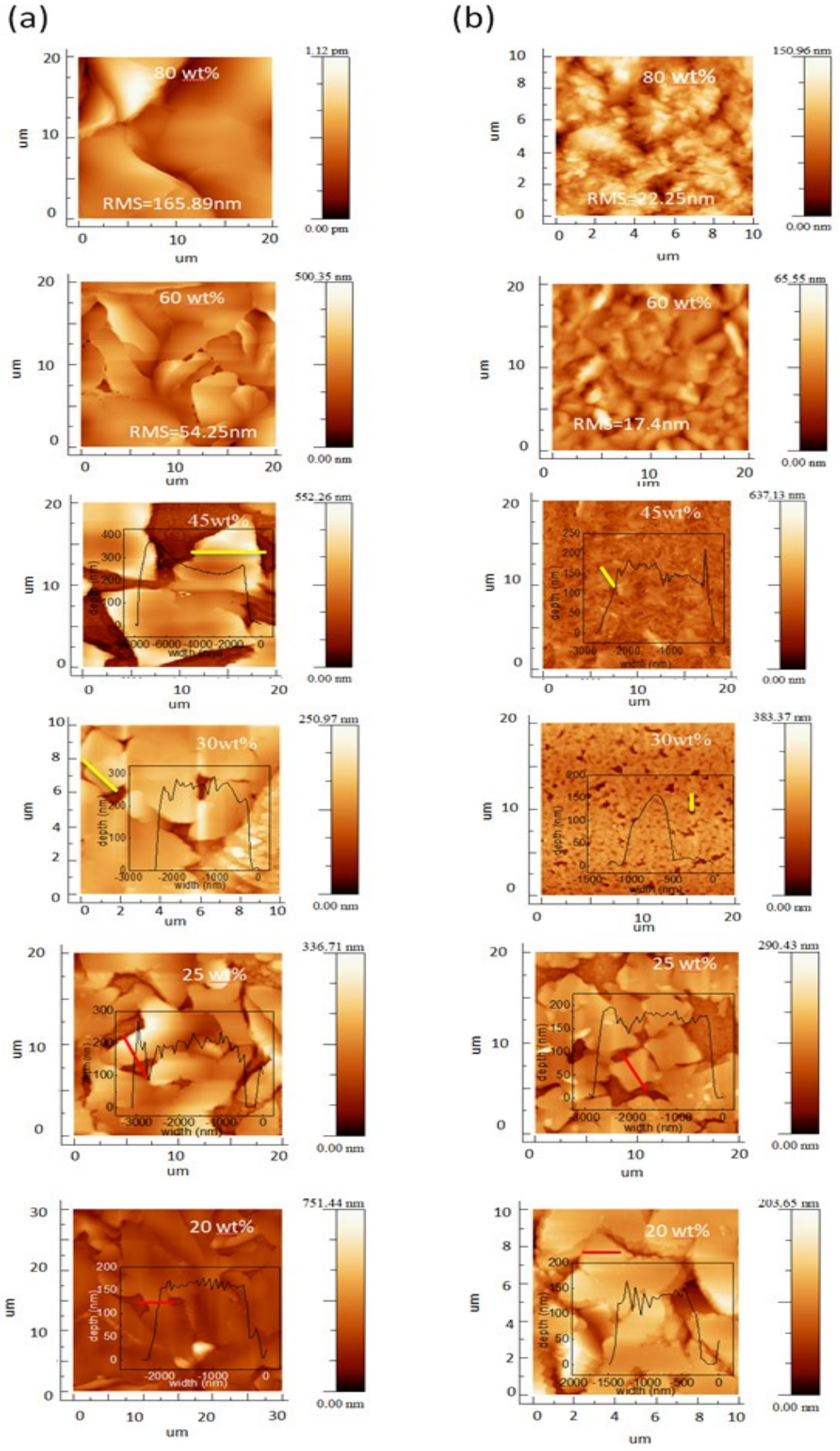

Figure S6: The AFM image of $(S\text{-}BA)_2PbI_4$ films(a) without and (b) with CB treatment for different concentration of chiral perovskite

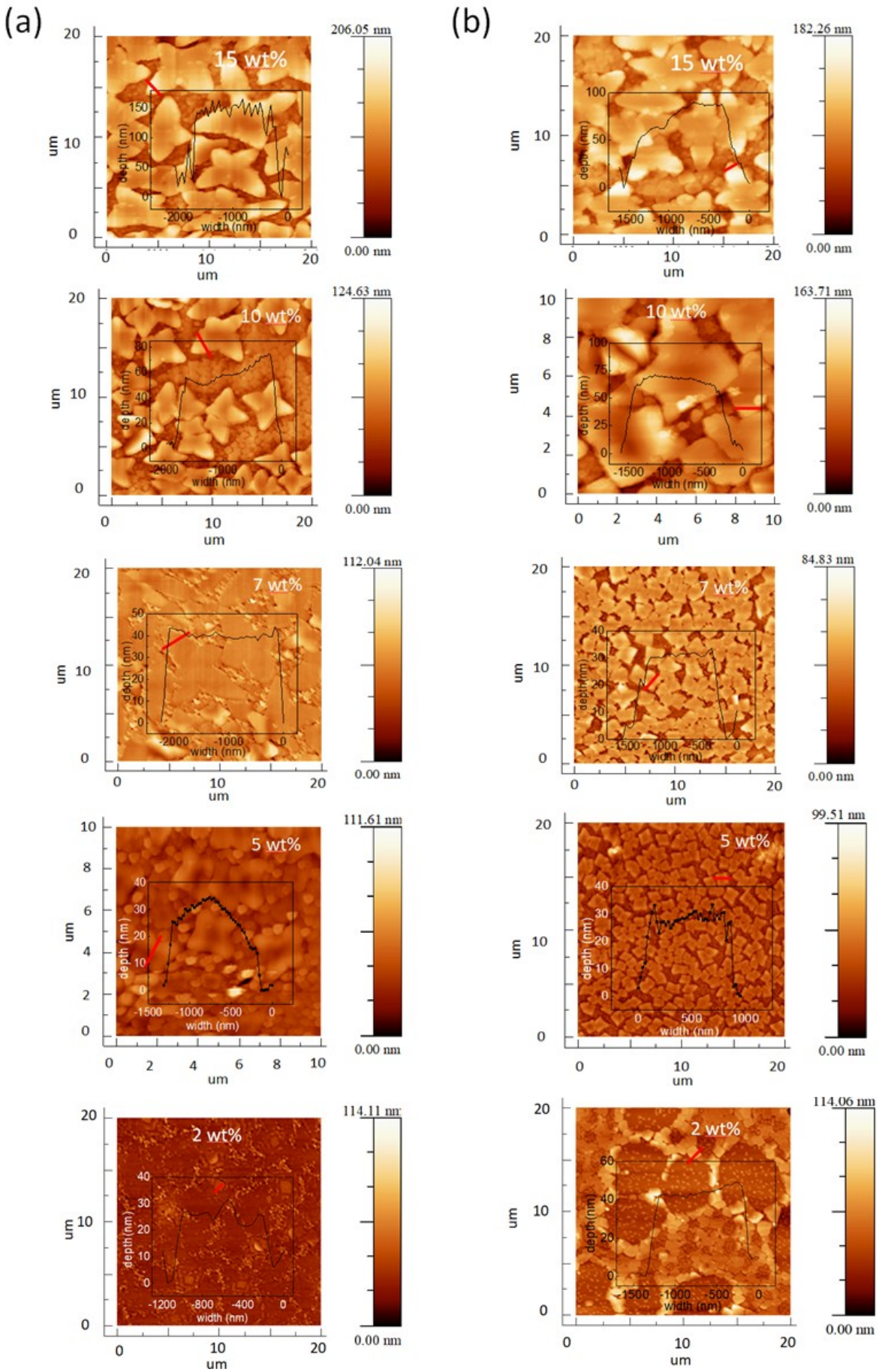

Figure S7: The AFM image of $(S\text{-}BA)_2PbI_4$ films (a) without and (b) with CB treatment for different concentration of chiral perovskite.

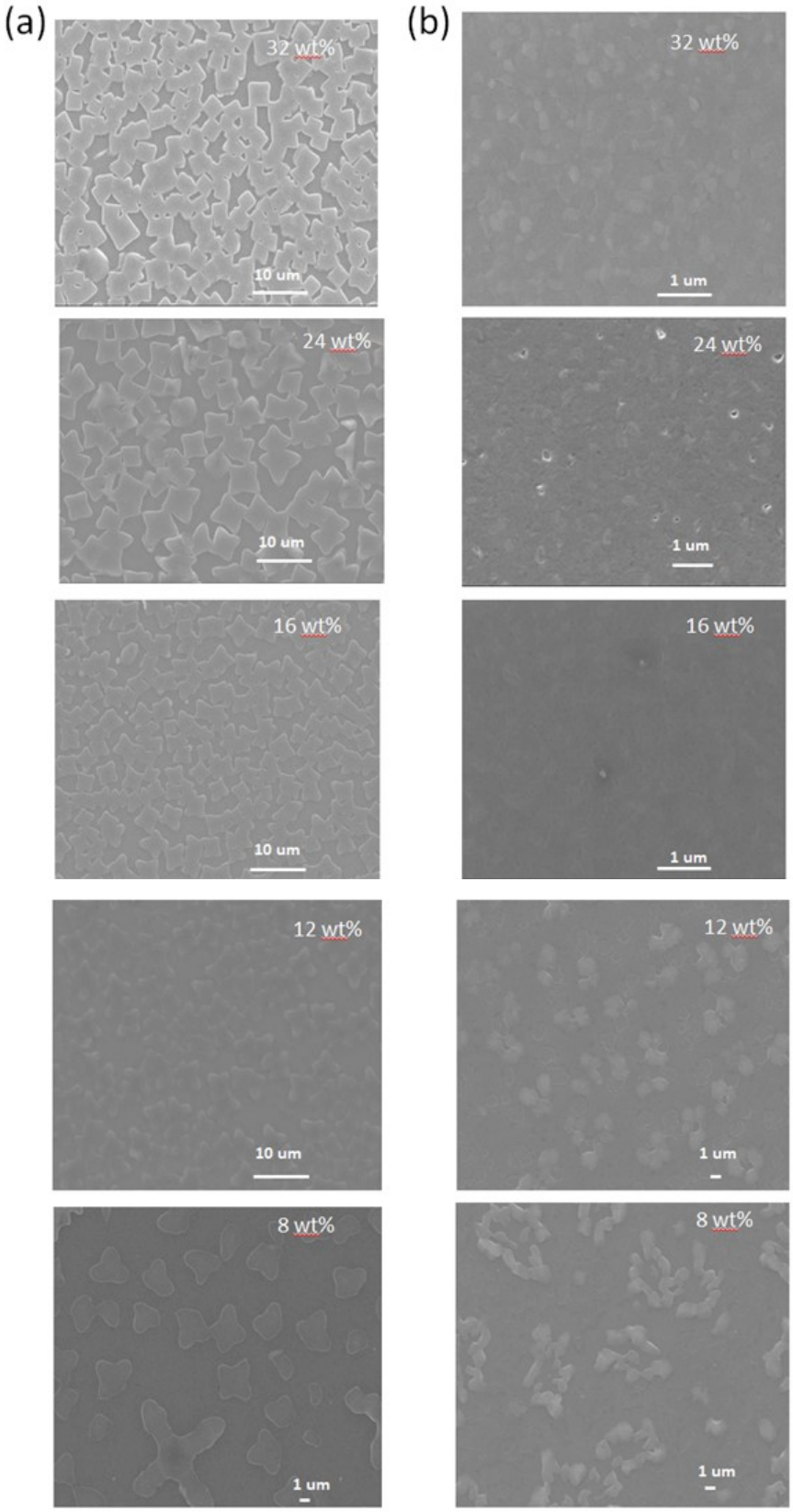

Figure S8: The top view SEM image of $(S\text{-}BA)_2PbBr_4$ films (a) without and (b) with CB treatment for different concentration of chiral perovskite.

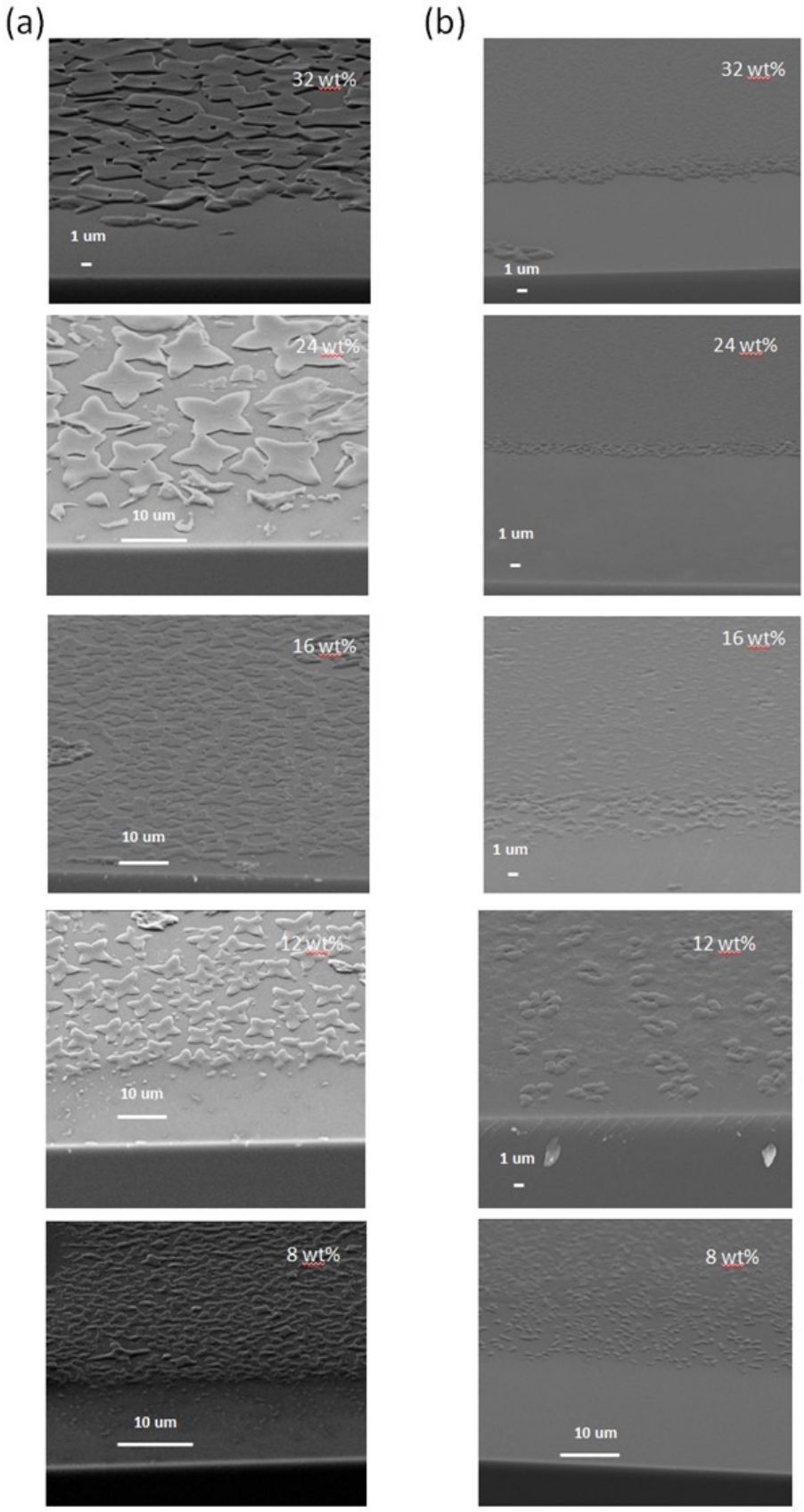

Figure S9: The incline view of SEM image of $(S\text{-}BA)_2PbBr_4$ films (a) without and (b) with CB treatment for different concentration of chiral perovskite.

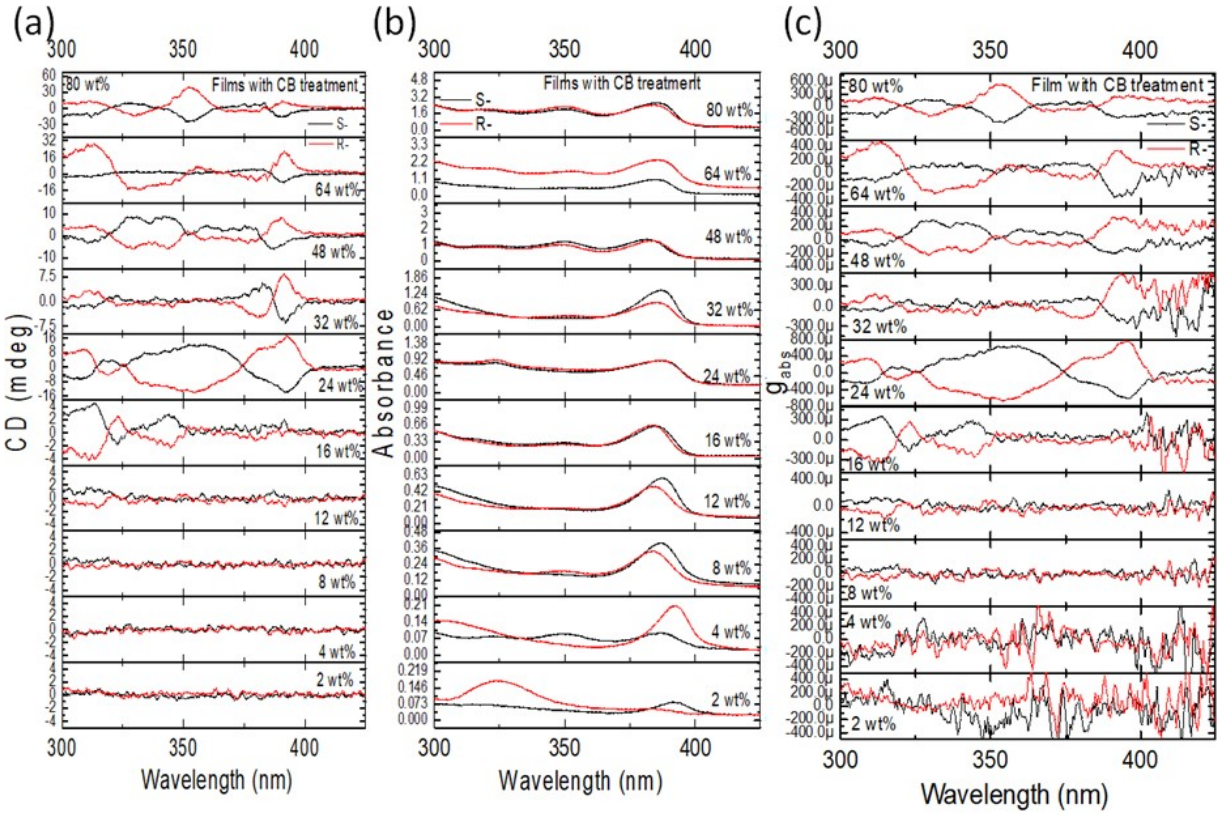

Figure S10: The(a) CD, (b)absorbance, and(c) gabs of the CB-treated (S-/R-BA)$_2$PbBr$_4$ films for different concentration of chiral perovskite

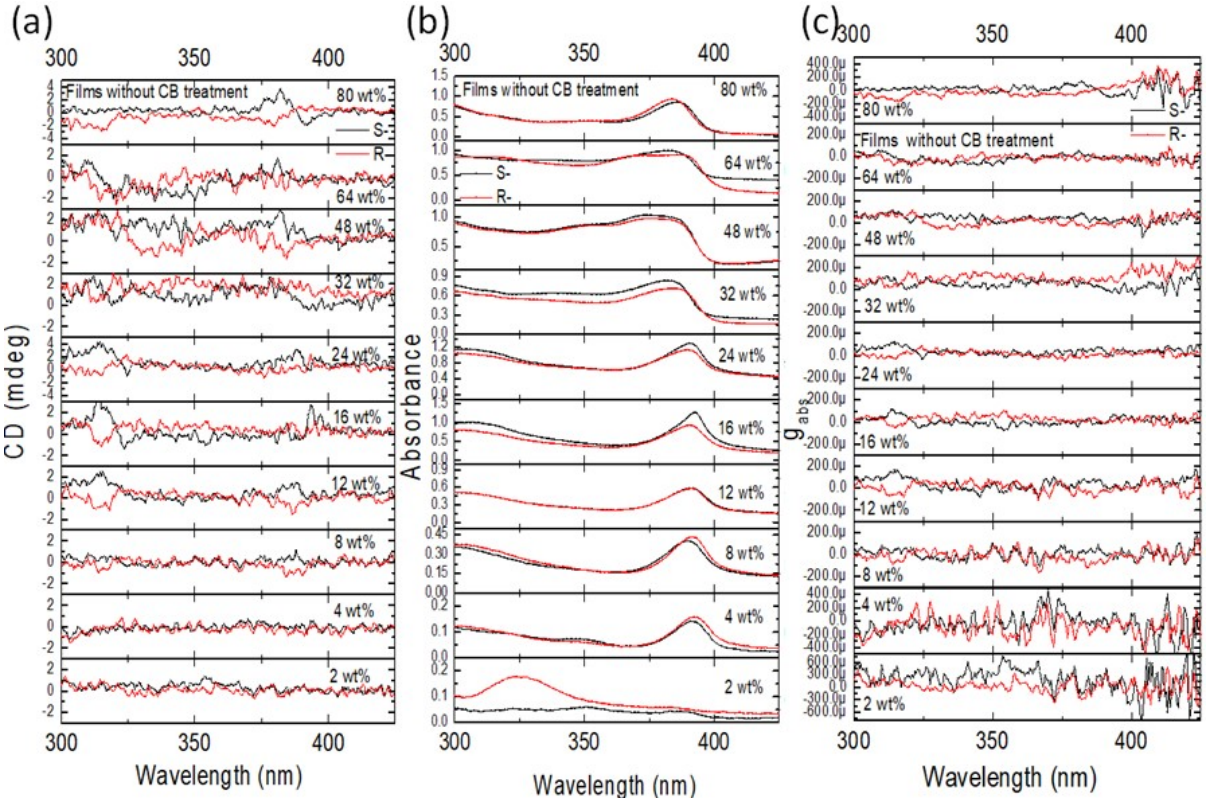

Figure S11: The(a) CD, (b)absorbance, and(c) gabs of the untreated(S-/R-BA)$_2$PbBr$_4$ films for different concentration of chiral perovskite.

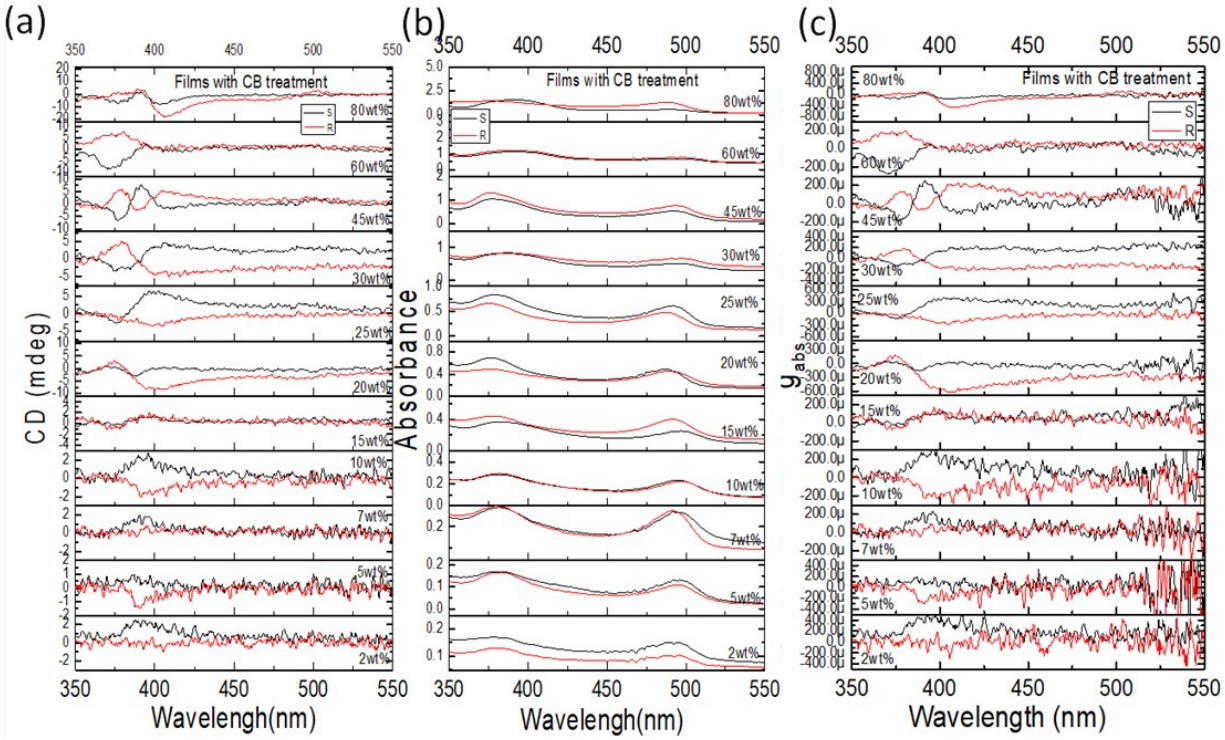

Figure S12: The (a) CD,(b) absorbance, and(c) gabs of the CB-treated (S-/R-BA)$_2$PbI$_4$ films for different concentration of chiral perovskite

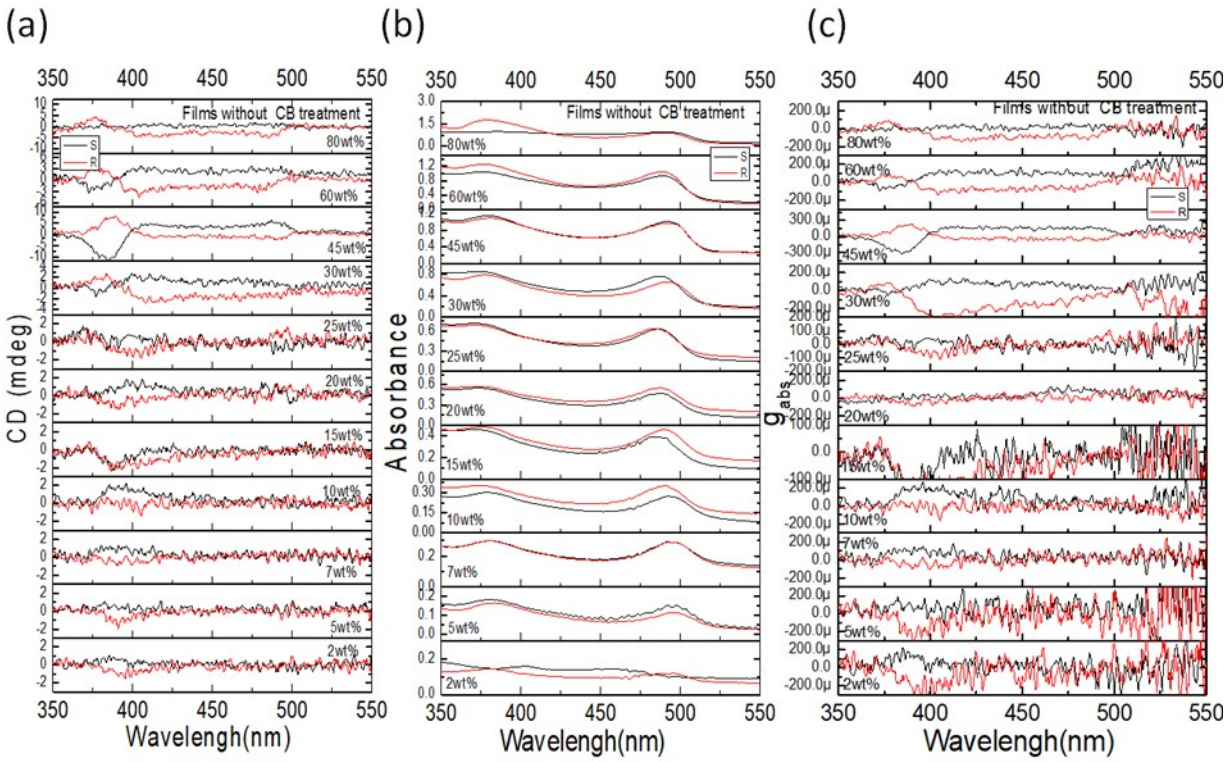

Figure S13: The (a) CD, (b)absorbance, and(c) gabs of the untreated(S-/R-BA)$_2$PbI$_4$ films for different concentration of chiral perovskite

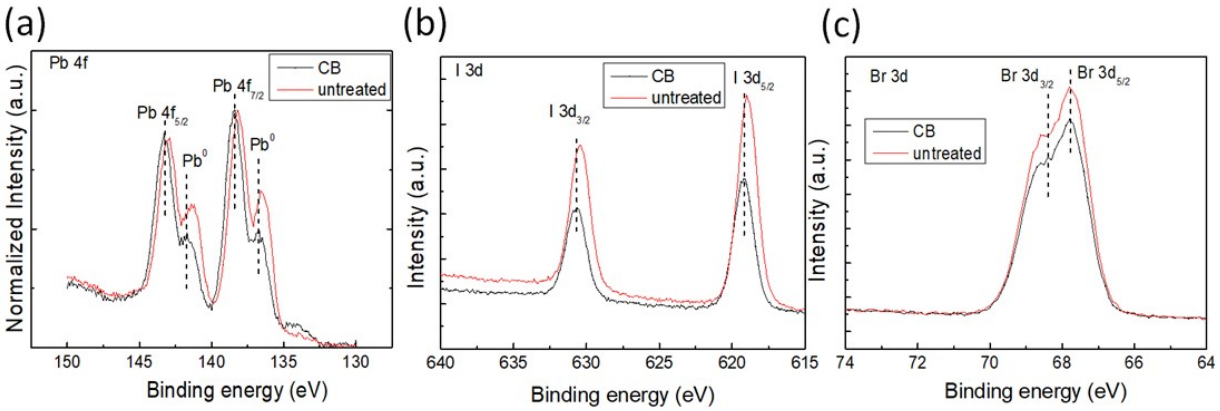

Figure S14: High-resolution XPS of (a) Pb 4f, (b) I 3d, and Br 3d peaks for the untreated and CF-treated films.

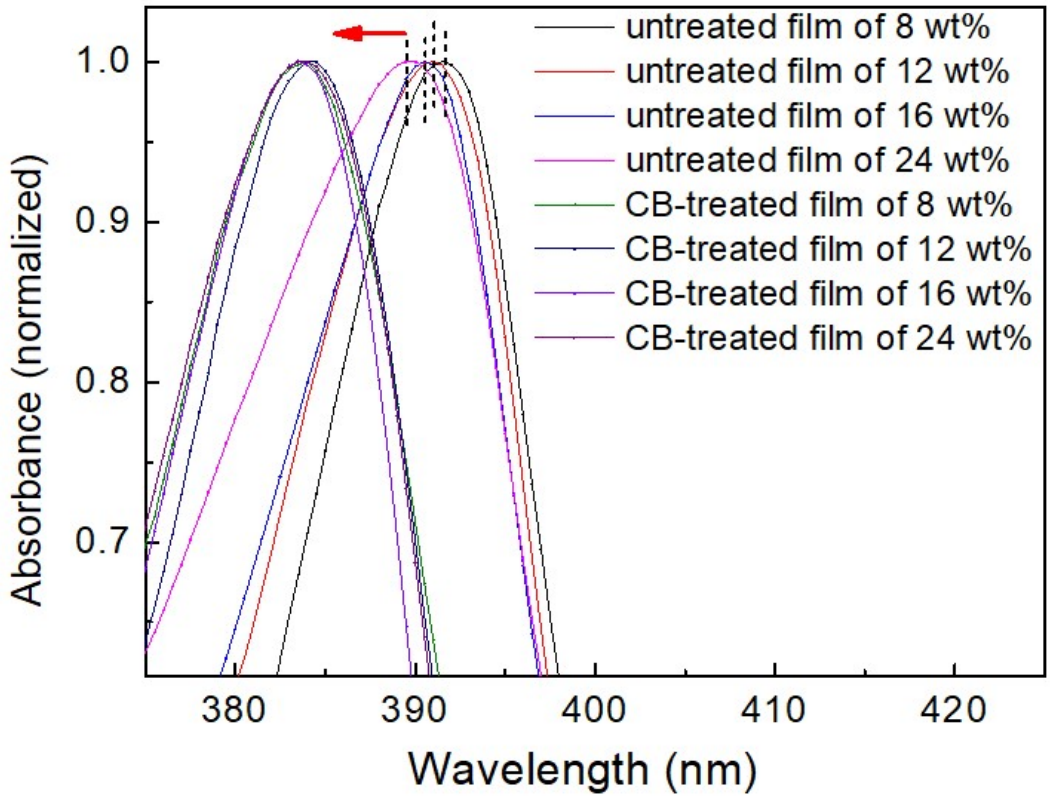

Figure S15: UV-vis absorption spectra of the CB-treated and untreated (R-BA)$_2$PbBr$_4$ film with various concentration of 8 wt%, 12wt%, 16wt% and 24wt%.

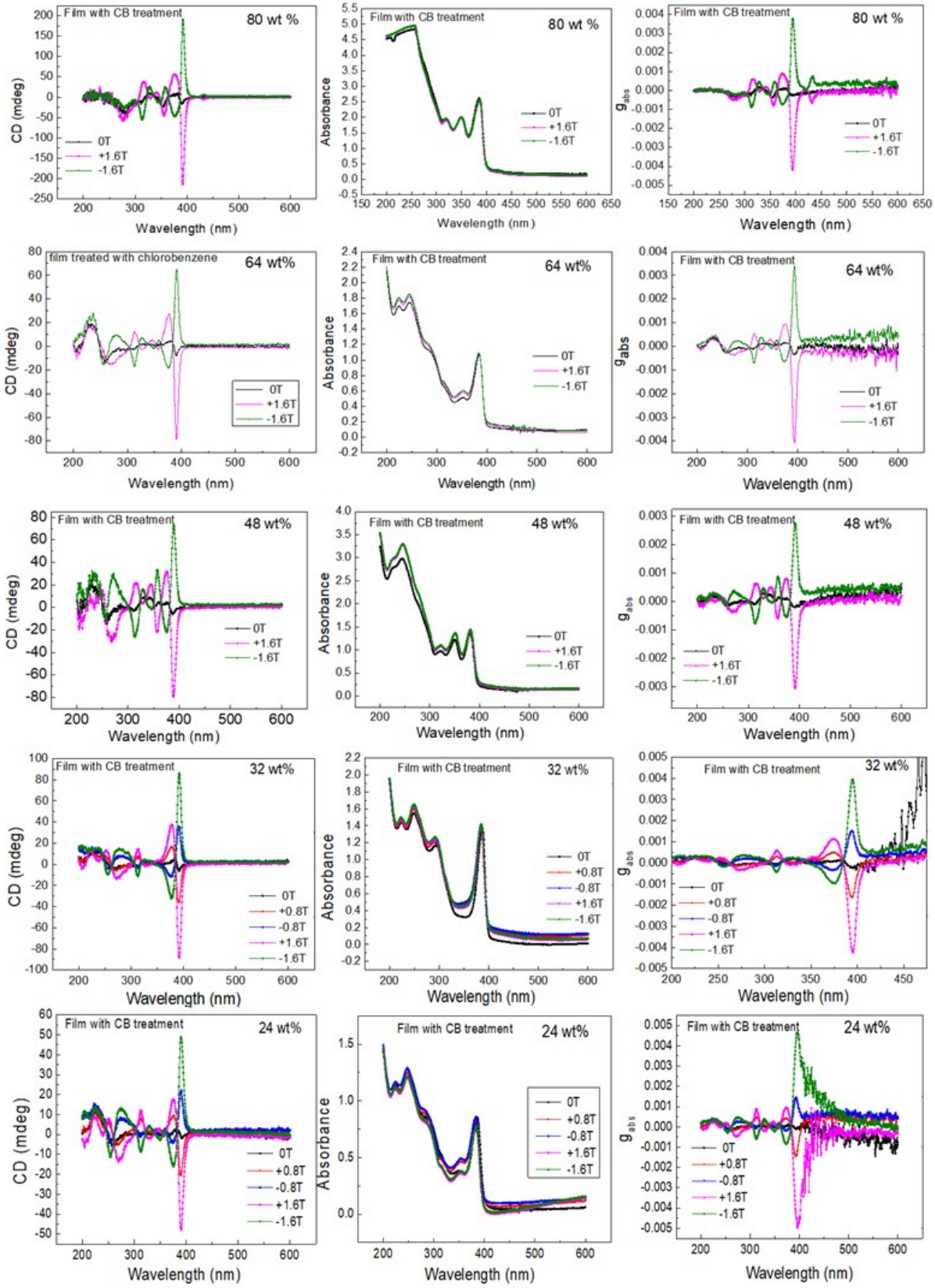

Figure S16: The CD, absorbance, and gabs of the CB-treated $(S\text{-}BA)_2PbBr_4$ films with CB treatment for different concentrations of chiral perovskite at the presence of a magnetic field.

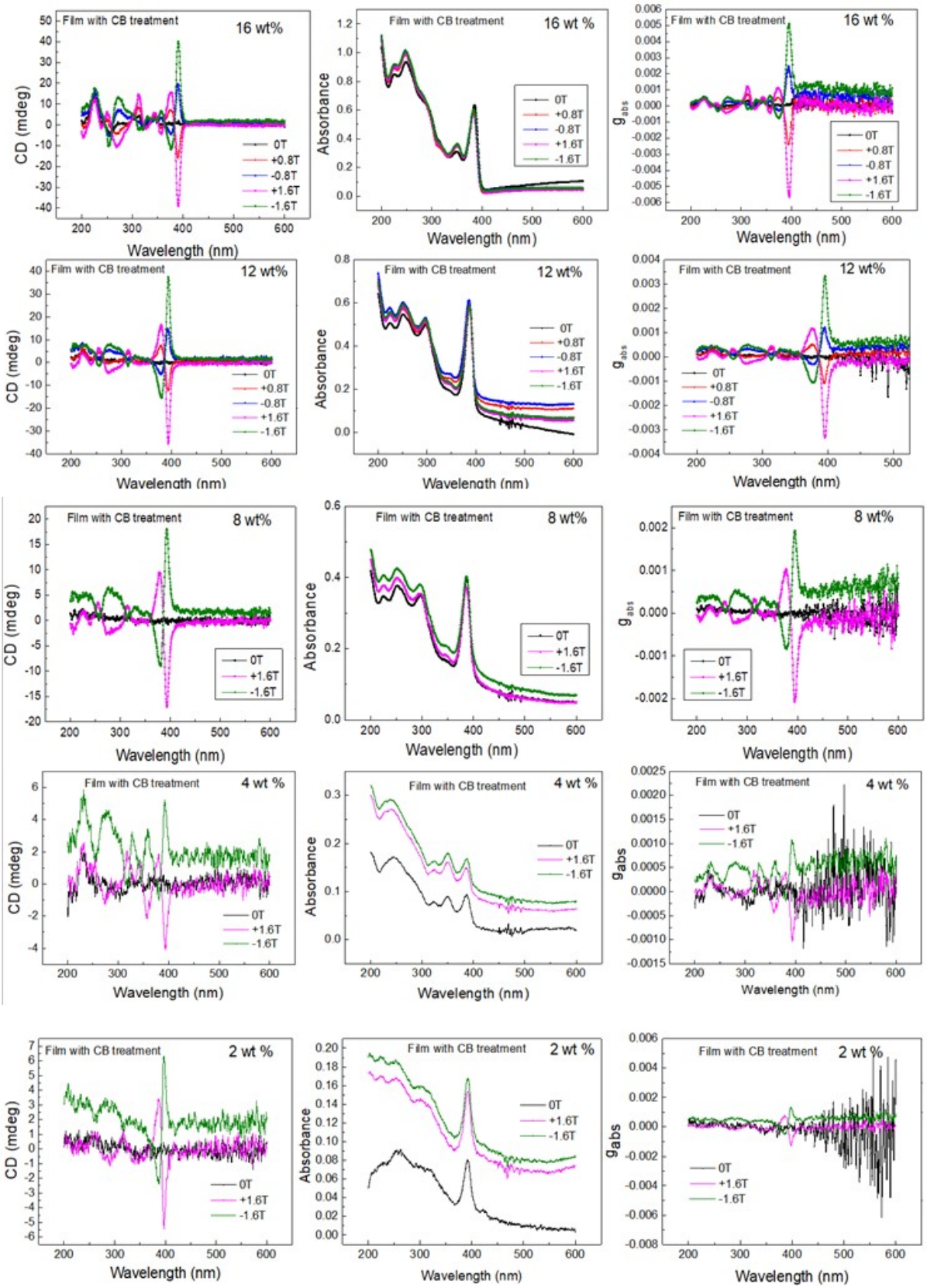

Figure S17: The CD, absorbance, and gabs of $(S\text{-}BA)_2PbBr_4$ films with CB treatment for different concentrations of chiral perovskite at the presence of a magnetic field

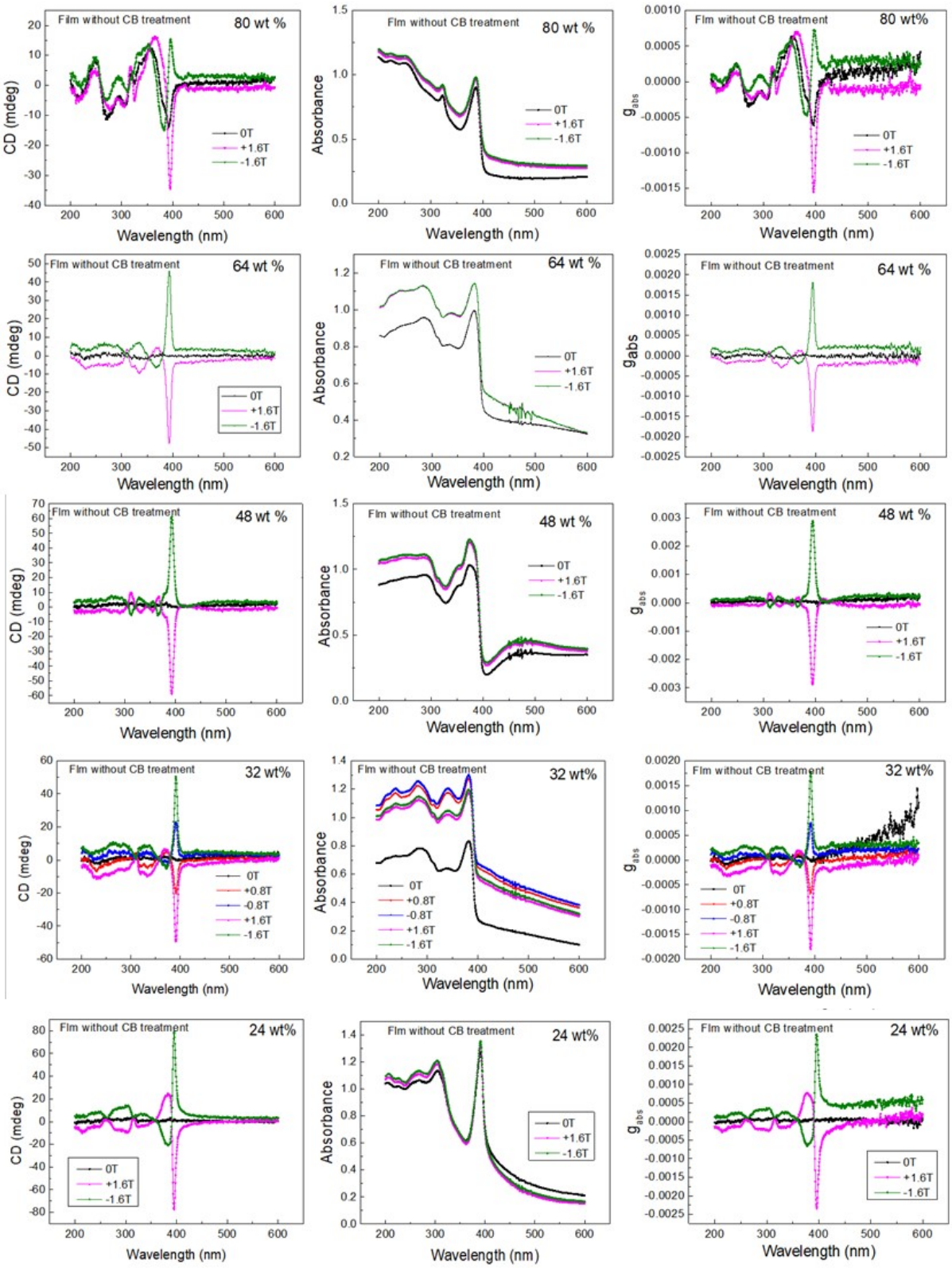

Figure S18: The CD, absorbance, and gabs of $(S\text{-}BA)_2PbBr_4$ films without CB treatment for different concentrations of chiral perovskite at the presence of a magnetic field

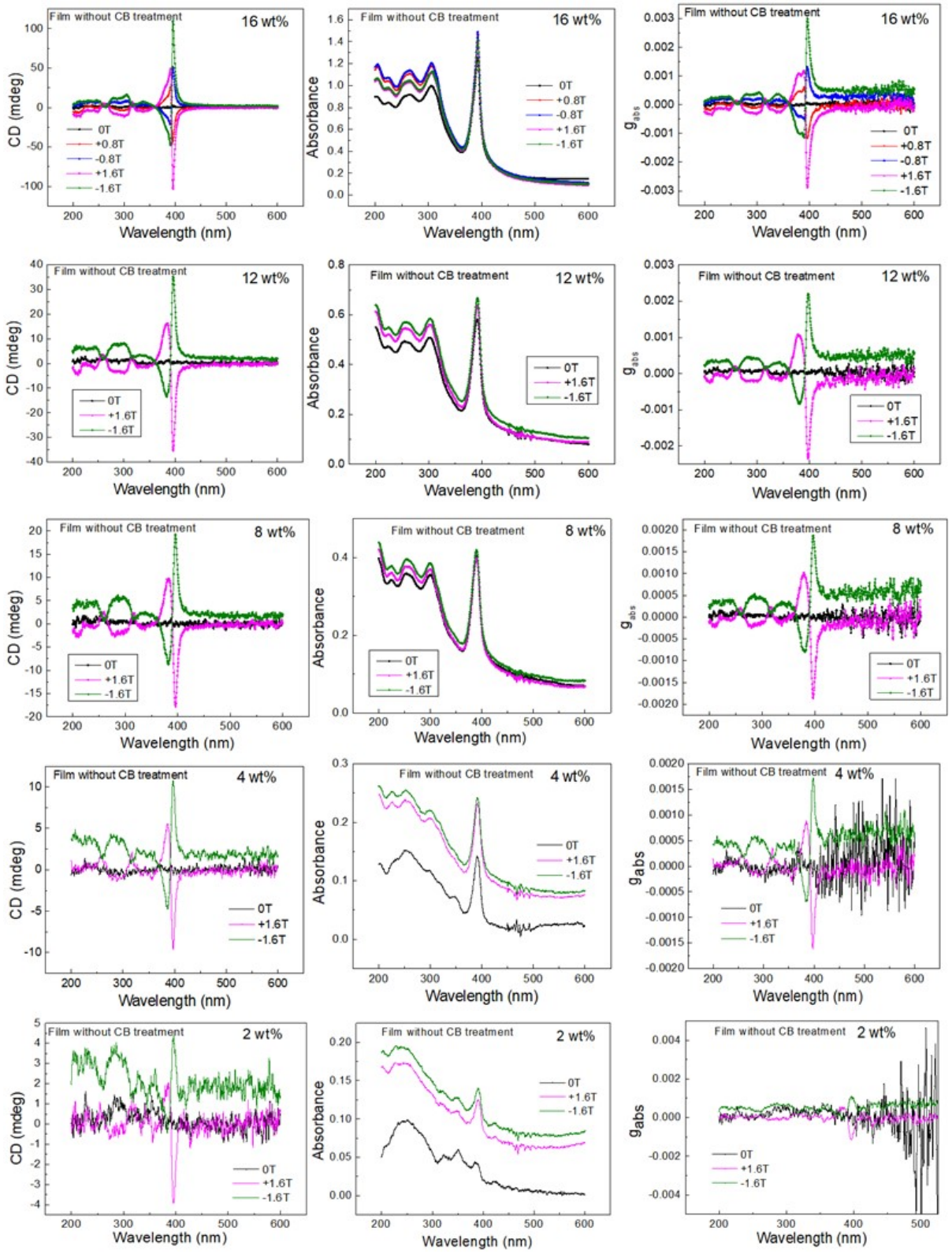

Figure S19: The CD, absorbance, and gabs of $(S\text{-}BA)_2PbBr_4$ films without CB treatment for different concentrations of chiral perovskite at the presence of a magnetic field

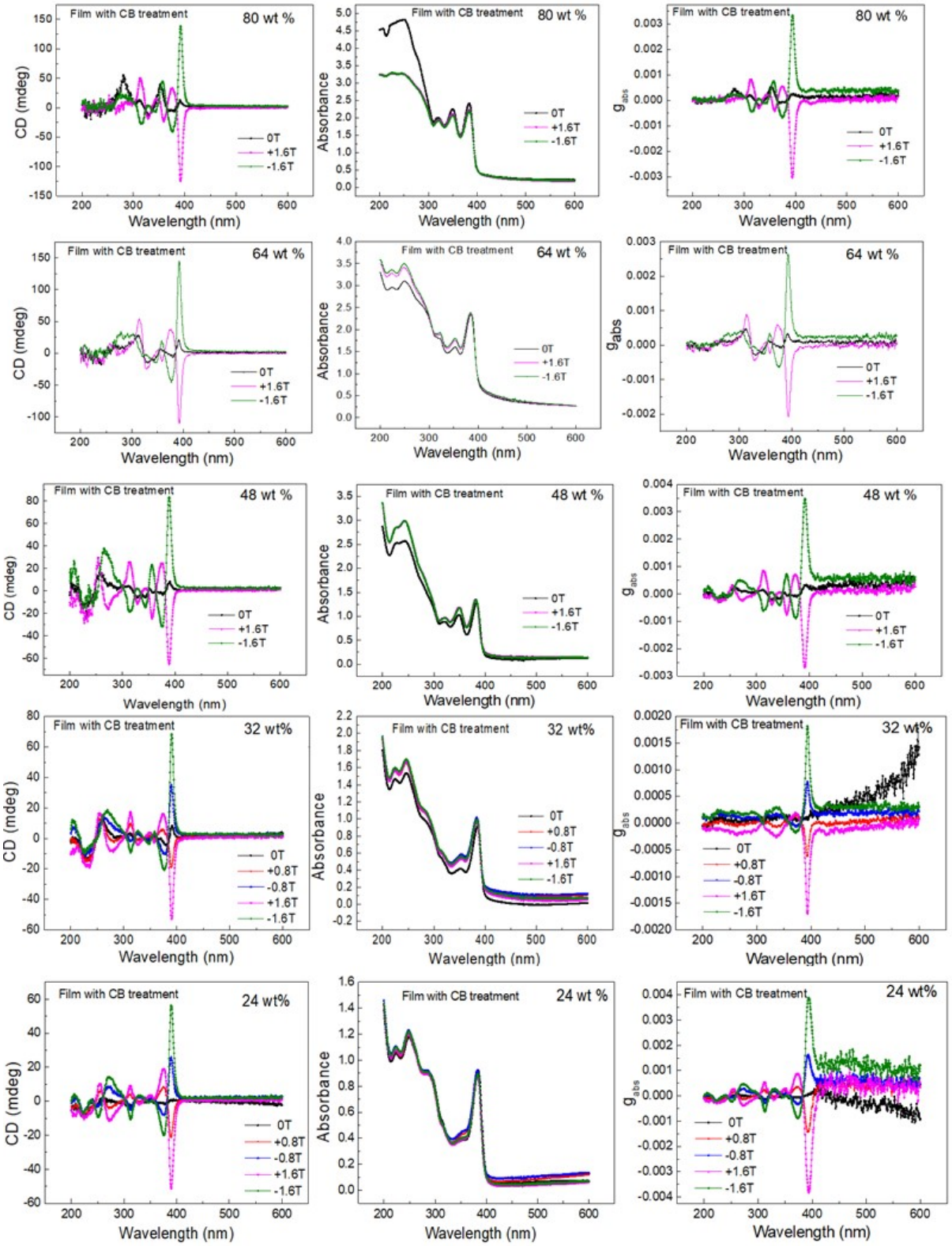

Figure S20: The CD, absorbance, and gabs of $(R\text{-}BA)_2PbBr_4$ films with CB treatment for different concentrations of chiral perovskite at the presence of a magnetic field

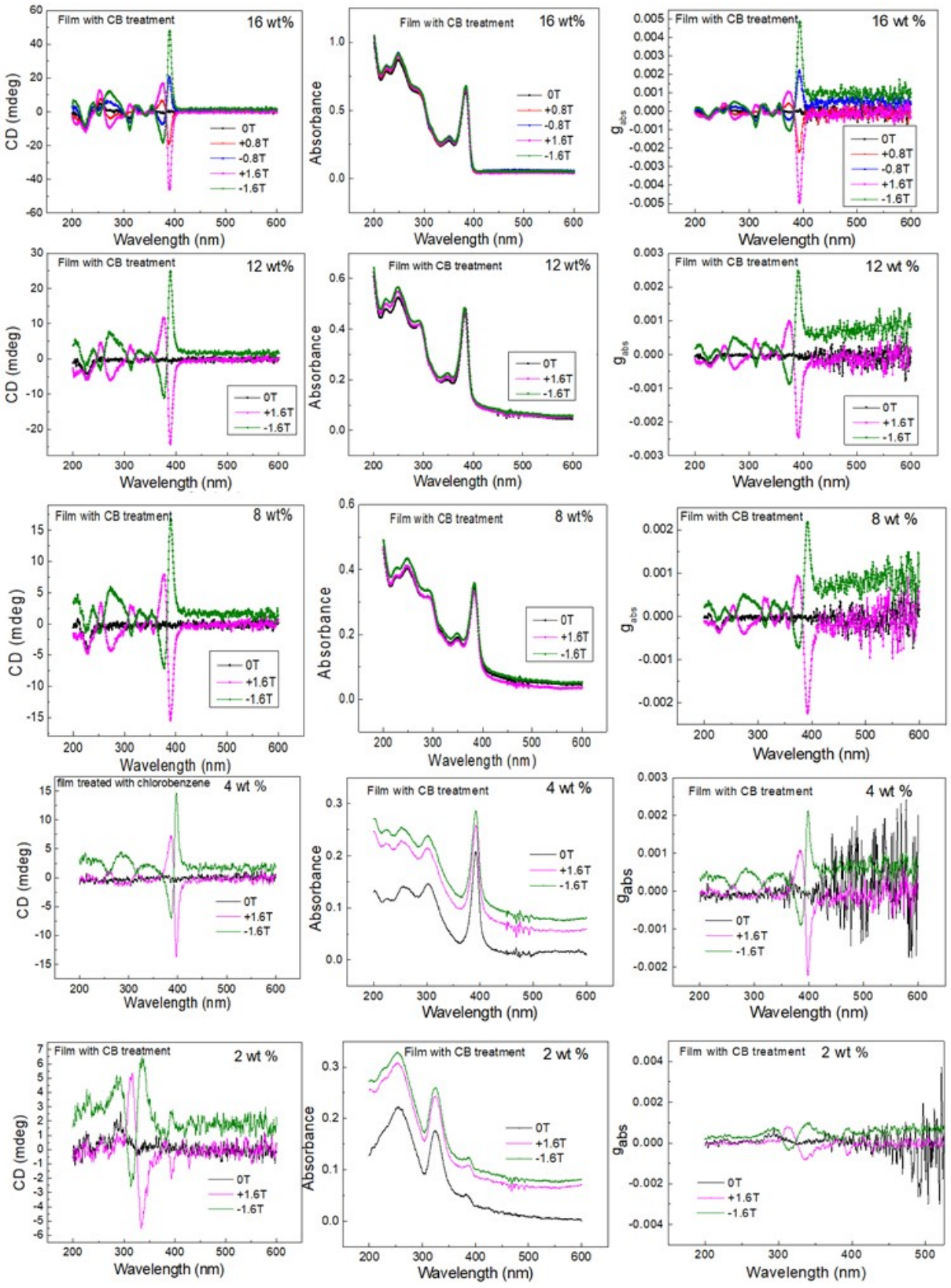

Figure S21: The CD, absorbance, and gabs of $(R\text{-}BA)_2PbBr_4$ films with CB treatment for different concentrations of chiral perovskite at the presence of a magnetic field

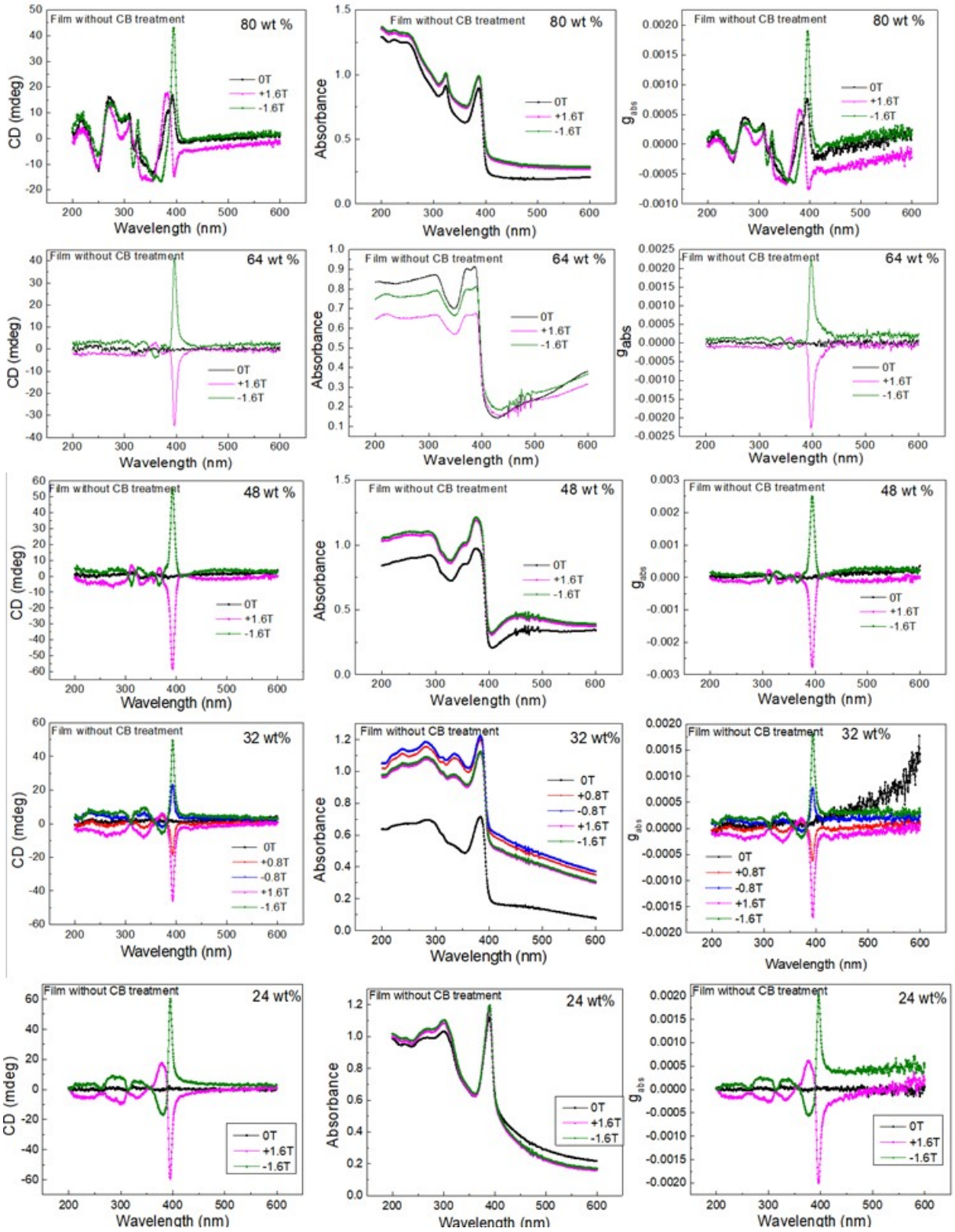

Figure S22: The CD, absorbance, and gabs of $(R\text{-}BA)_2PbBr_4$ films without CB treatment for different concentrations of chiral perovskite at the presence of a magnetic field

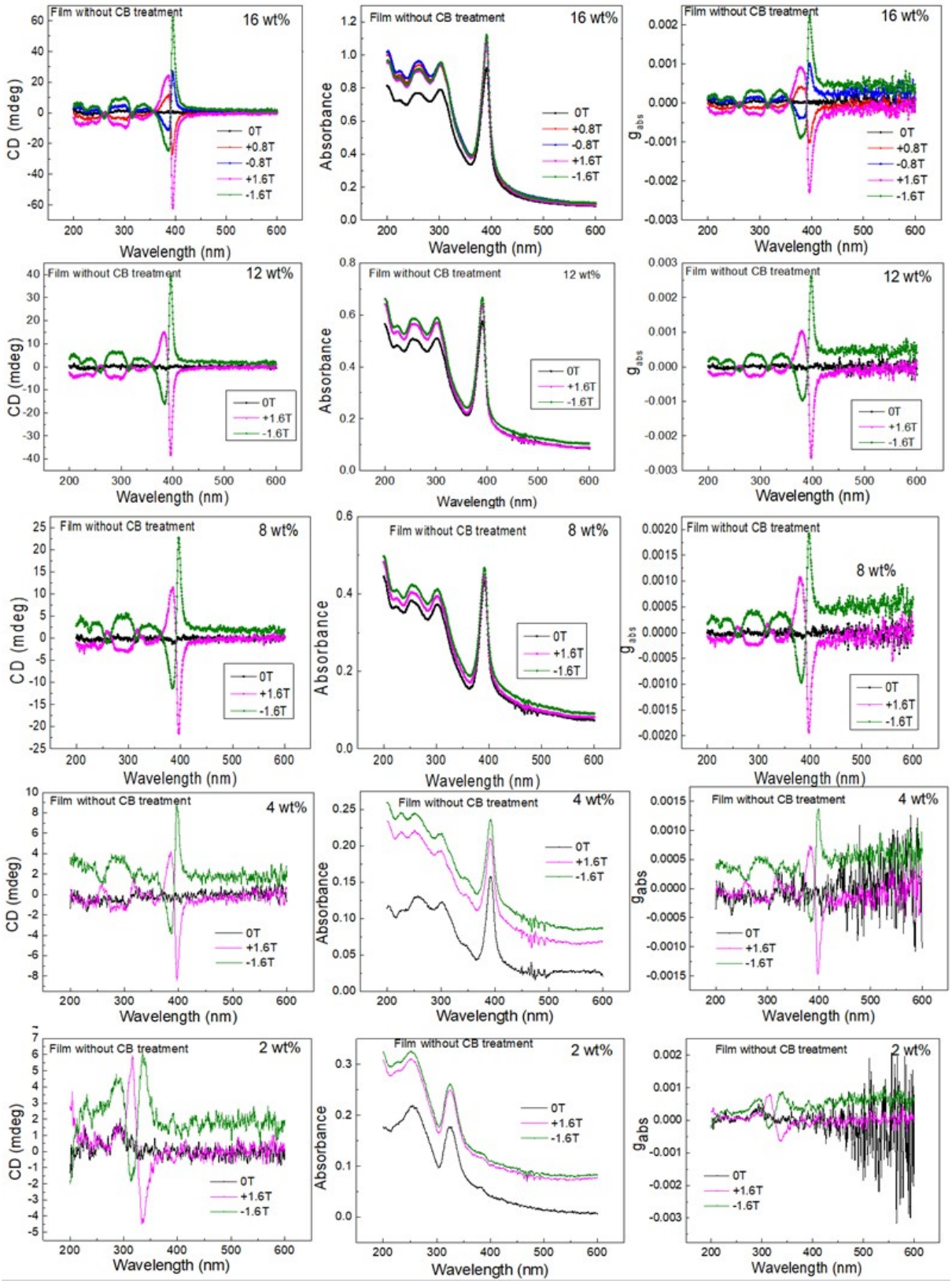

Figure S23: The CD, absorbance, and gabs of $(R\text{-}BA)_2PbBr_4$ films without CB treatment for different concentrations of chiral perovskite at the presence of a magnetic field

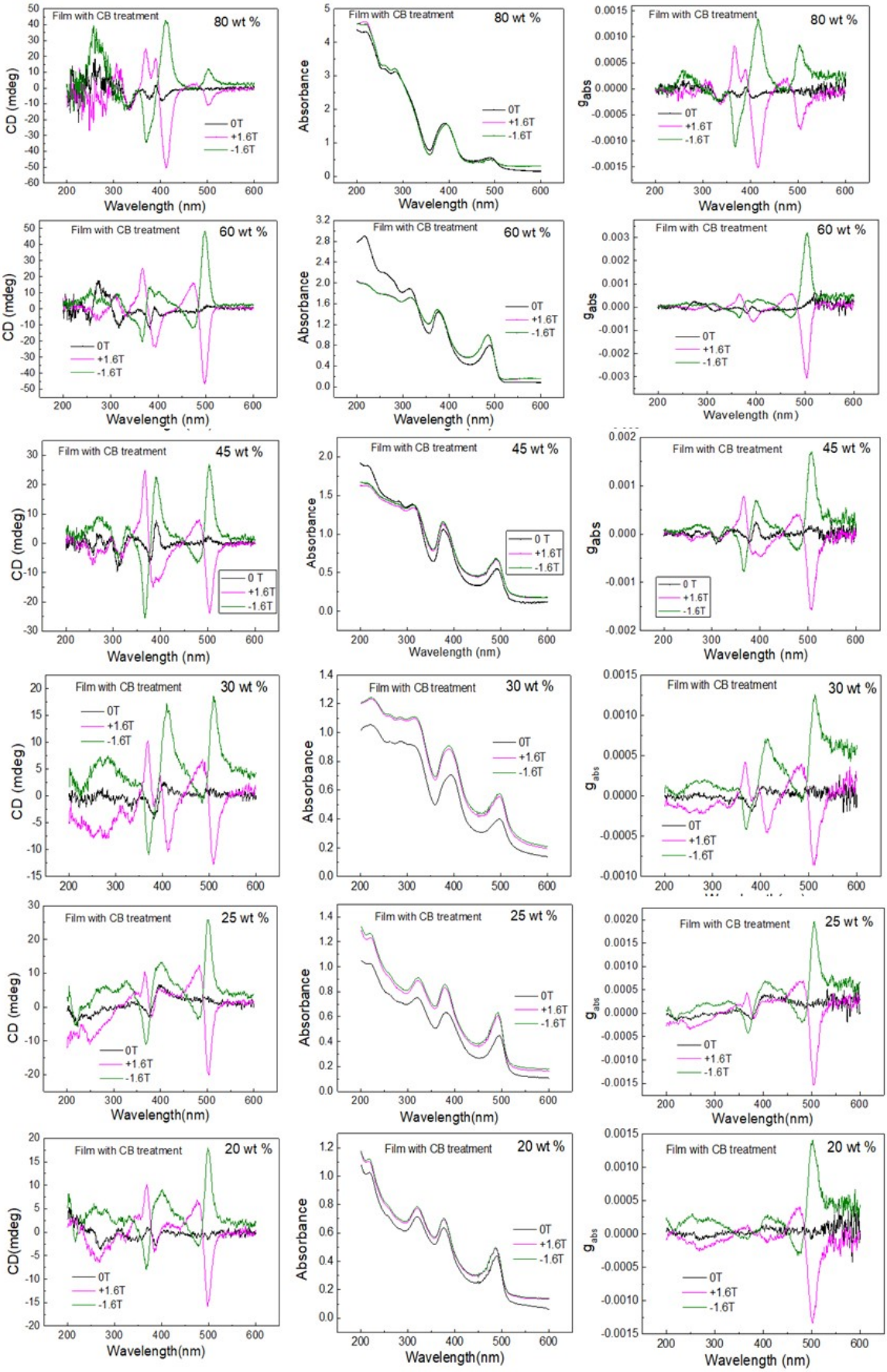

Figure S24: The CD, absorbance, and gabs of $(S\text{-}BA)_2PbI_4$ films with CB treatment for different concentrations of chiral perovskite at the presence of a magnetic field.

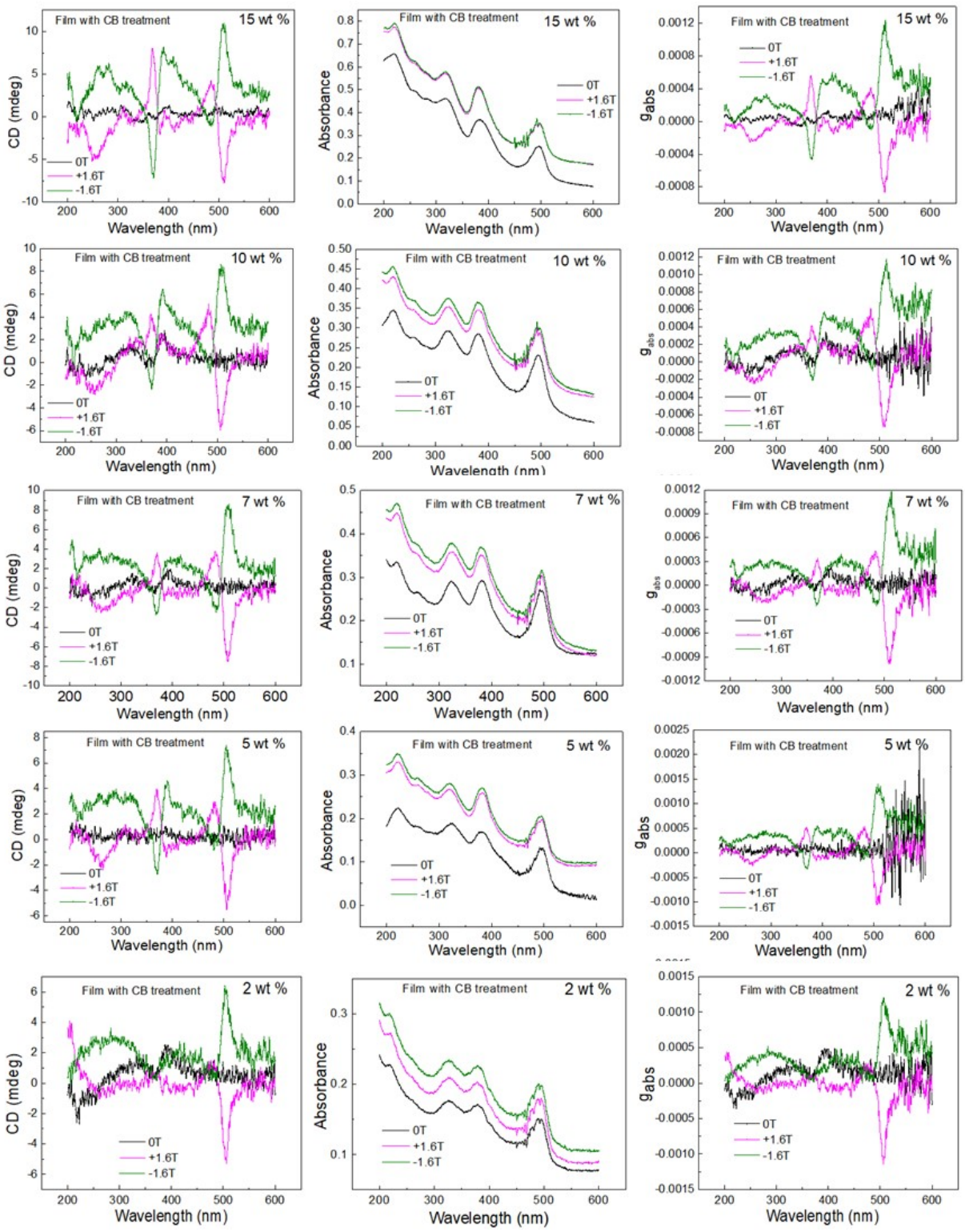

Figure S25: The CD, absorbance, and gabs of $(S\text{-}BA)_2PbI_4$ films with CB treatment for different concentrations of chiral perovskite at the presence of a magnetic field.

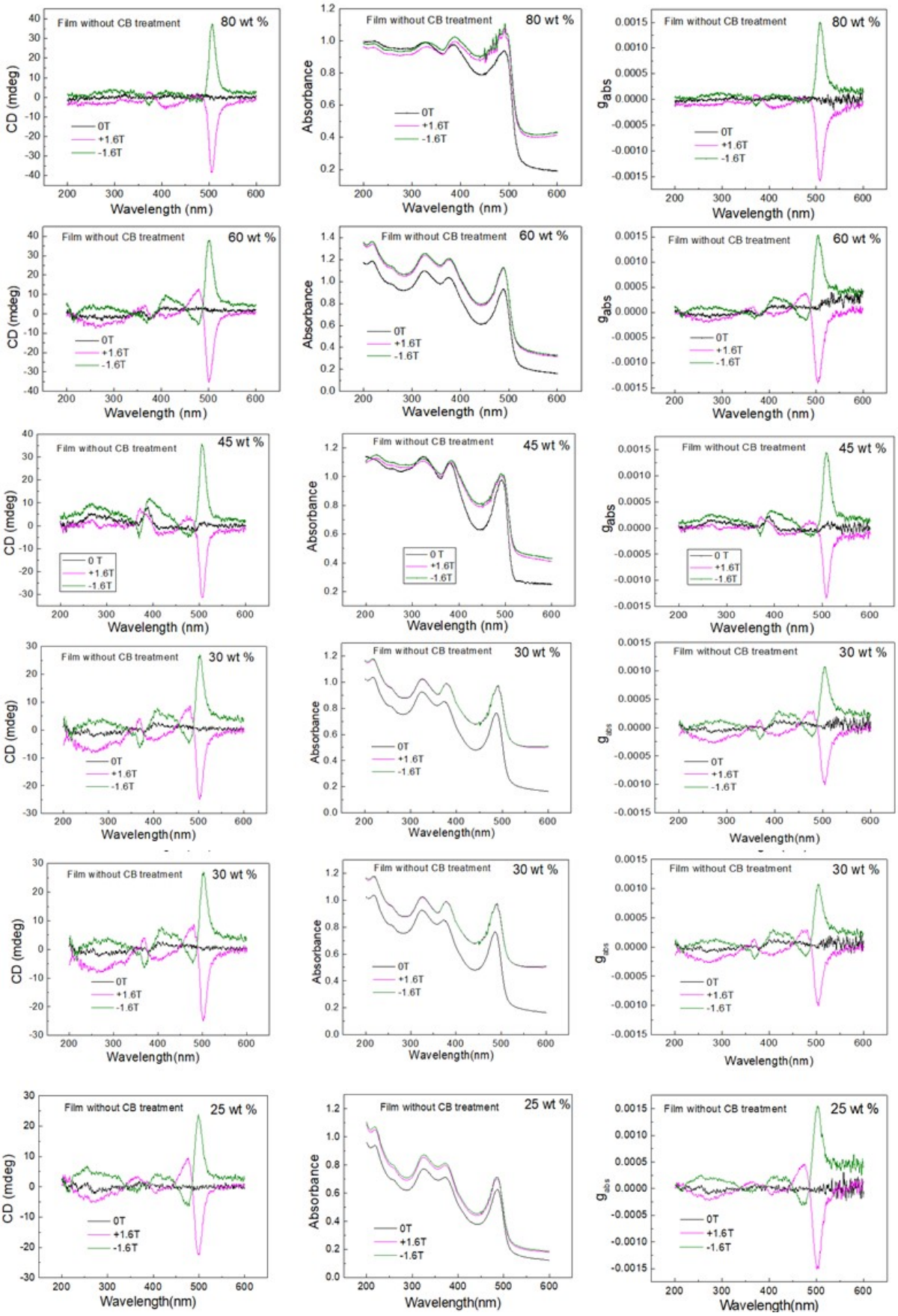

Figure S26: The CD, absorbance, and gabs of $(S\text{-}BA)_2PbI_4$ films without CB treatment for different concentrations of chiral perovskite at the presence of a magnetic field

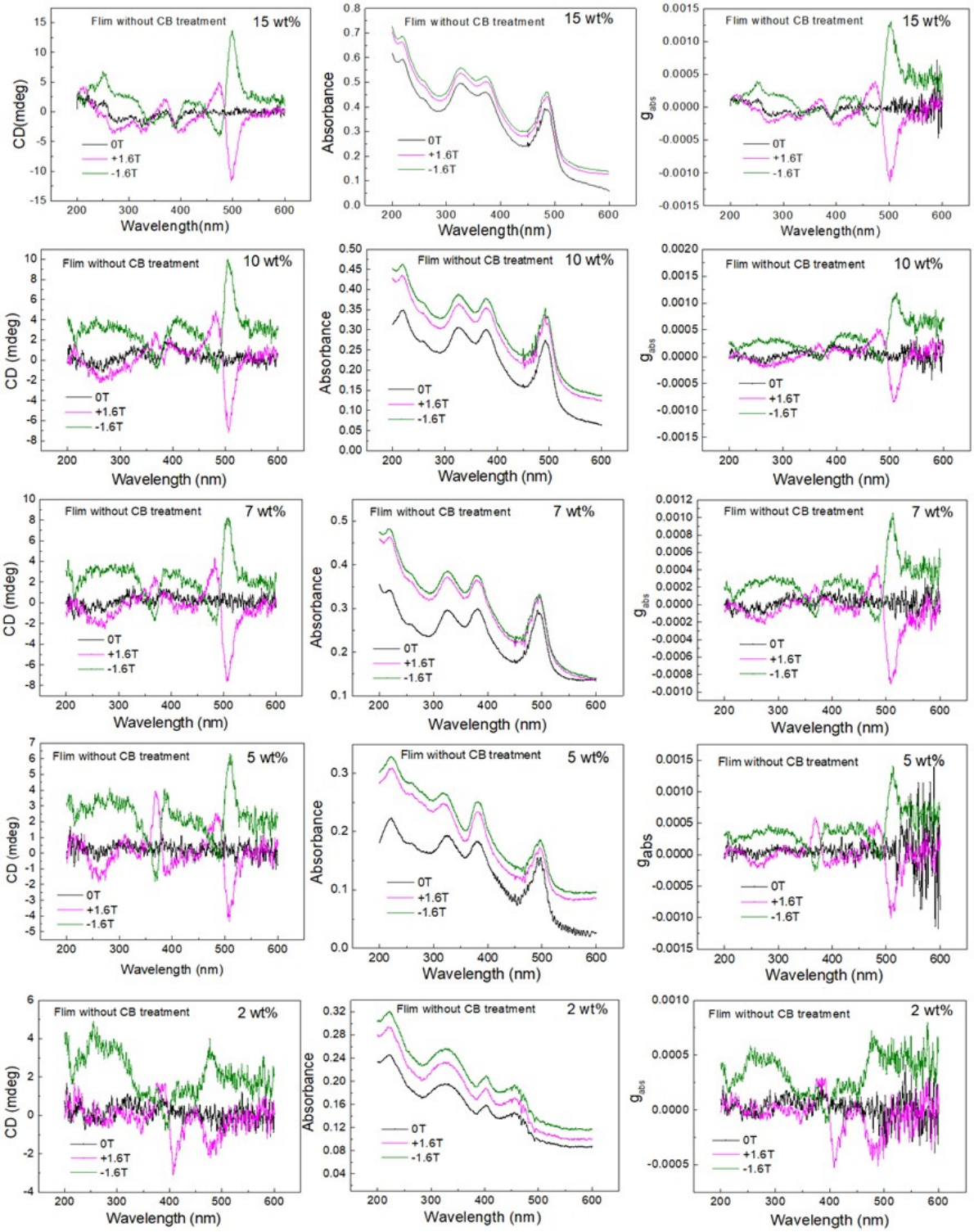

Figure S27: The CD, absorbance, and gabs of $(S\text{-}BA)_2PbI_4$ films without CB treatment for different concentrations of chiral perovskite at the presence of a magnetic field

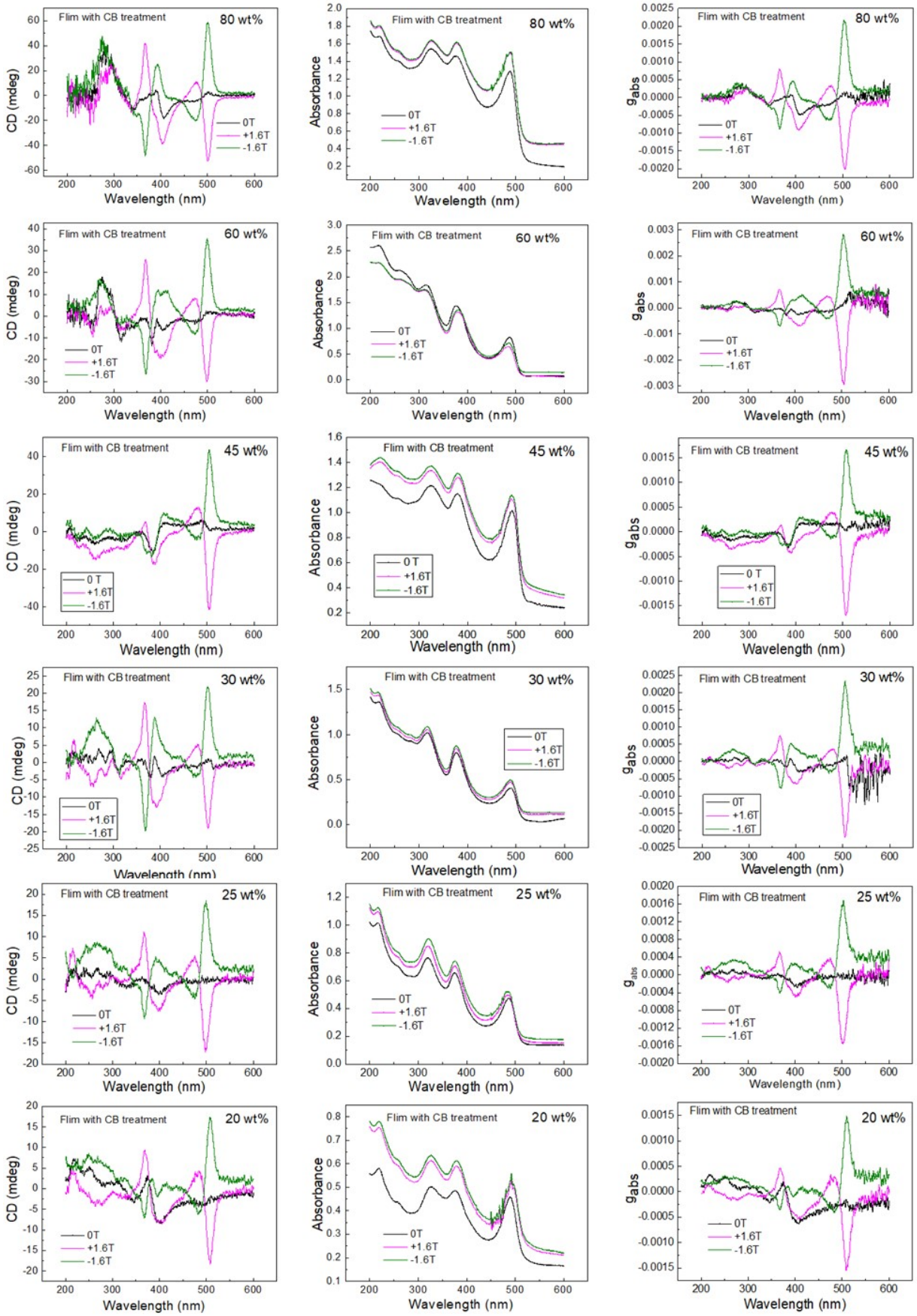

Figure S28: The CD, absorbance, and gabs of $(R\text{-}BA)_2PbI_4$ films with CB treatment for different concentrations of chiral perovskite at the presence of a magnetic field

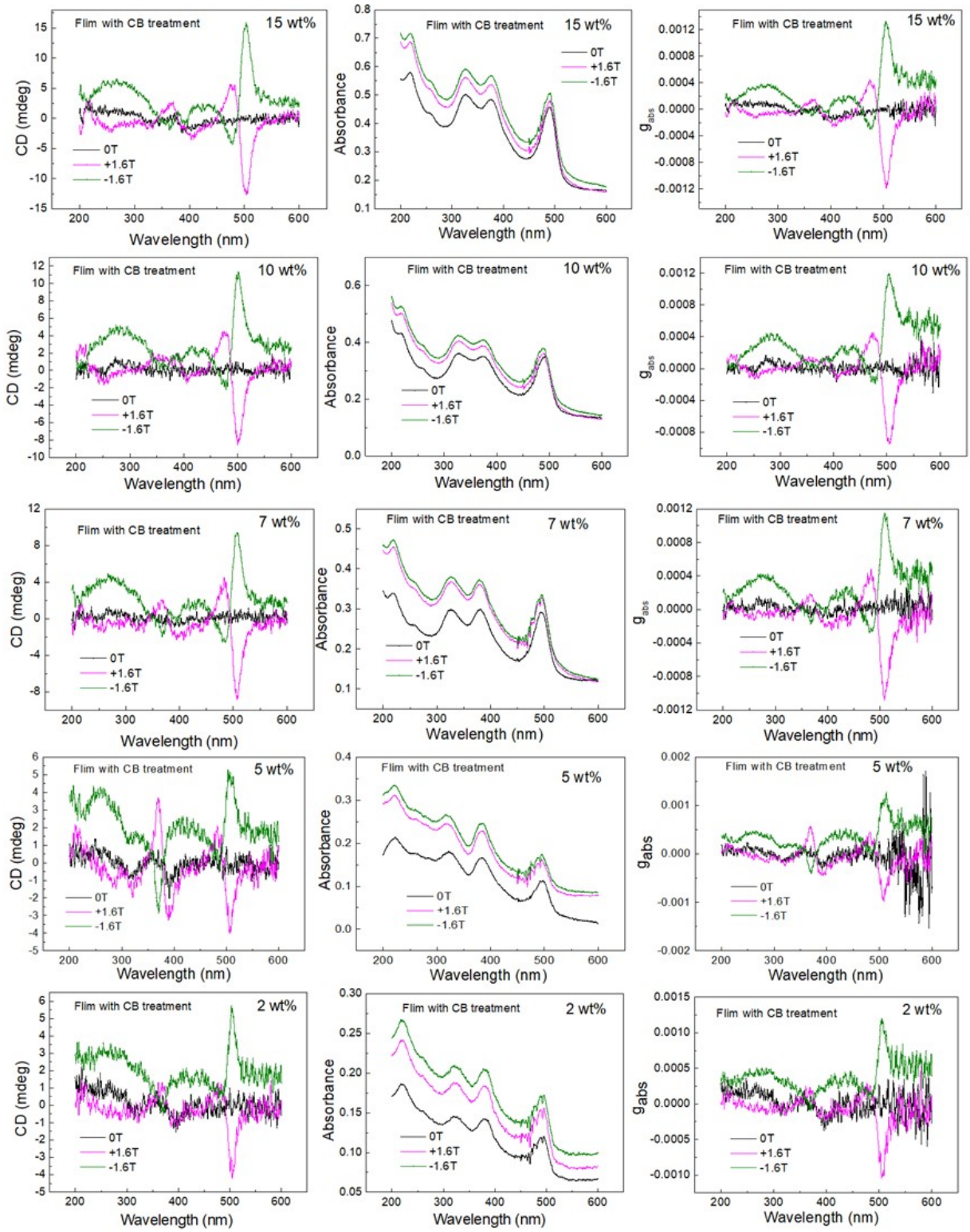

Figure S29: The CD, absorbance, and gabs of $(R\text{-}BA)_2PbI_4$ films with CB treatment for different concentrations of chiral perovskite at the presence of a magnetic field

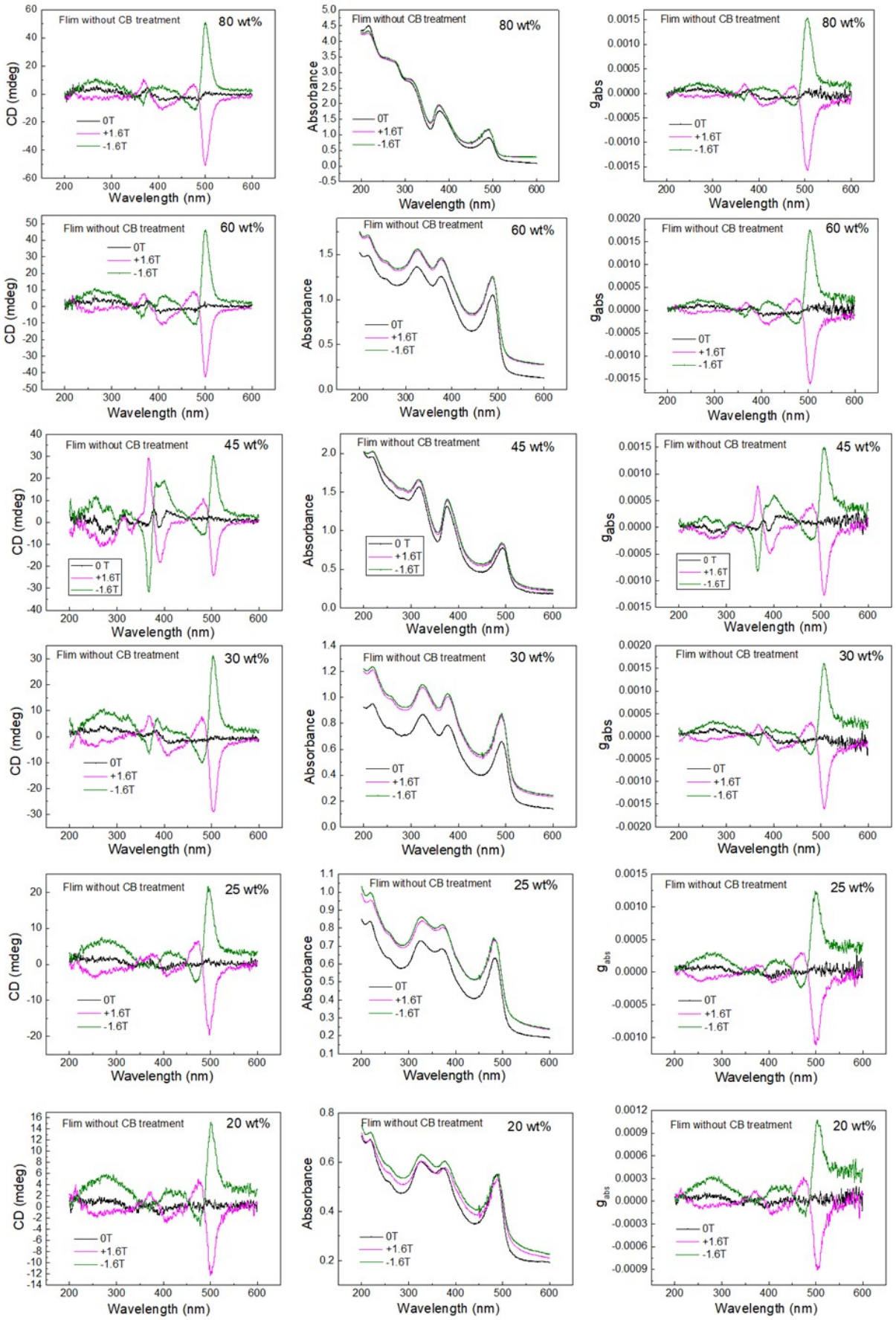

Figure S30: The CD, absorbance, and gabs of $(R\text{-}BA)_2PbI_4$ films without CB treatment for different concentrations of chiral perovskite at the presence of a magnetic field

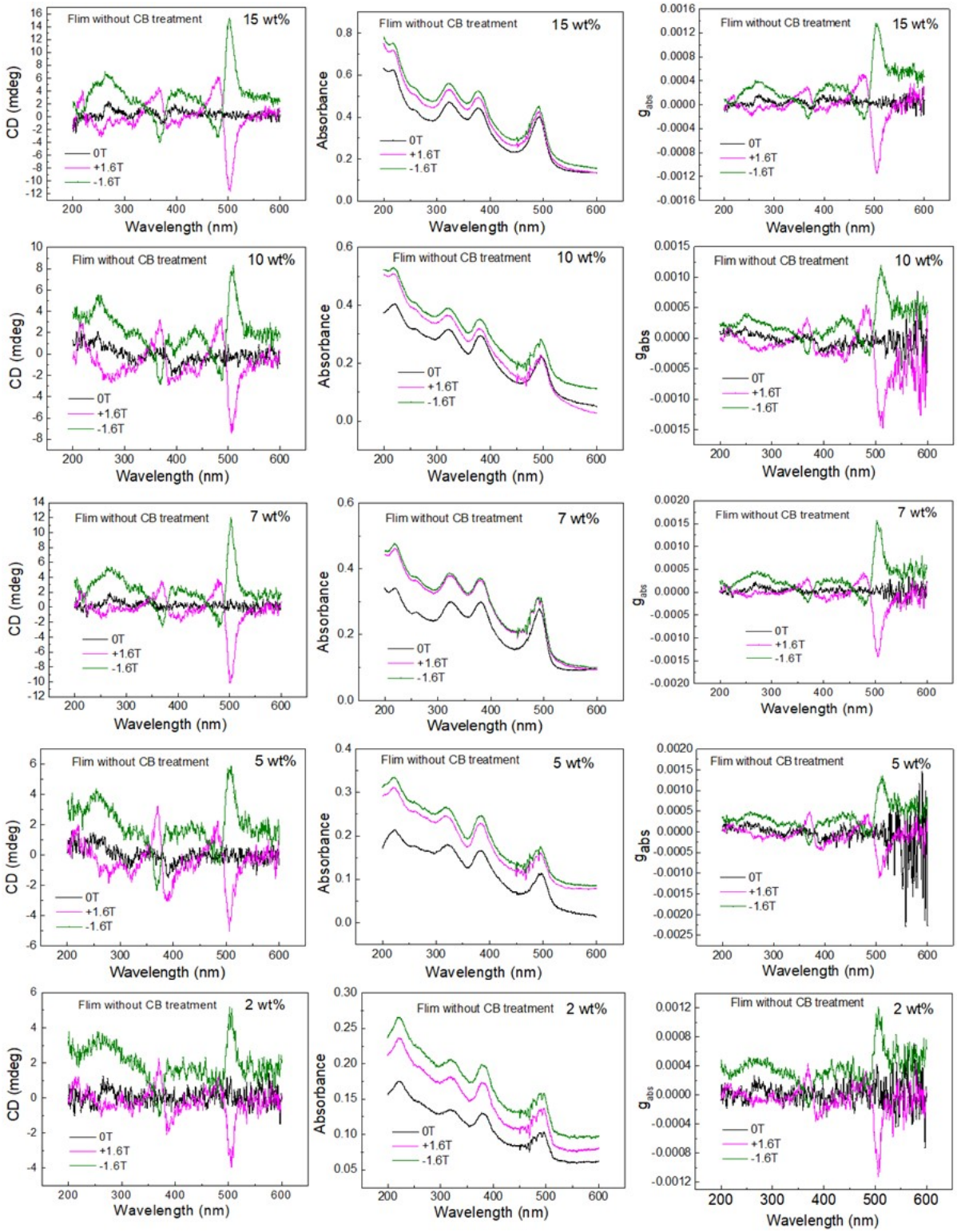

Figure S31: The CD, absorbance, and gabs of $(R\text{-}BA)_2PbI_4$ films without CB treatment for different concentrations of chiral perovskite at the presence of a magnetic field

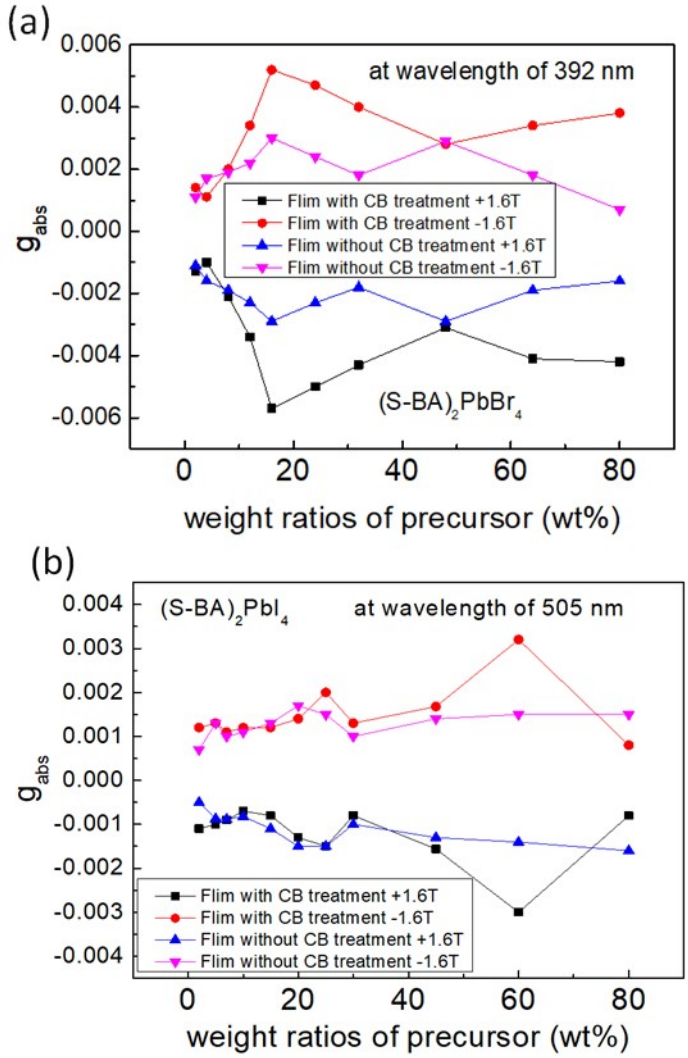

Figure S32: The gabs as a function of precursor concentration of (a) $(S\text{-}BA)_2PbBr_4$ and (b) $(S\text{-}BA)_2PbI_4$ films with CB treatment for different concentration of chiral perovskite

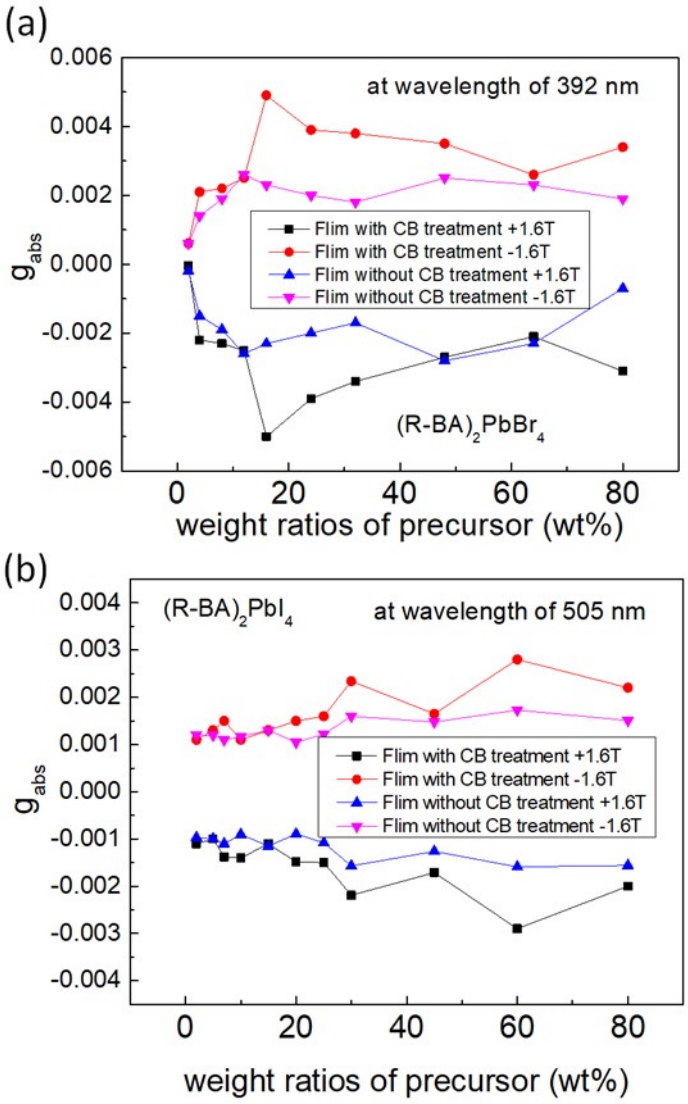

Figure S33: The gabs as a function of precursor concentration of(a) $(R\text{-}BA)_2PbBr_4$and (b) $(R\text{-}BA)_2PbI_4$films with and without CB treatment for different concentration of chiral perovskite.

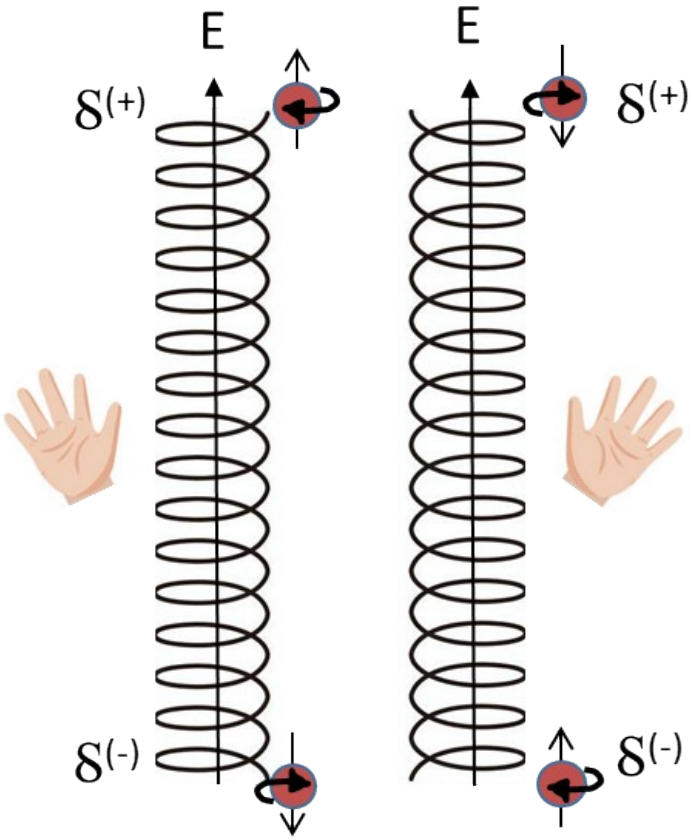

Figure S34: A schematic illustration of charge and spin polarization in a chiral molecule when the molecule is exposed to an electric field acting along its axis (black arrow). The electric field induces spin-selective electron movement, resulting in transient spin polarization at the poles (δ(+) and δ(−) at the ends of the helix). The spin correlated with each pole depends on the handedness of the molecule.

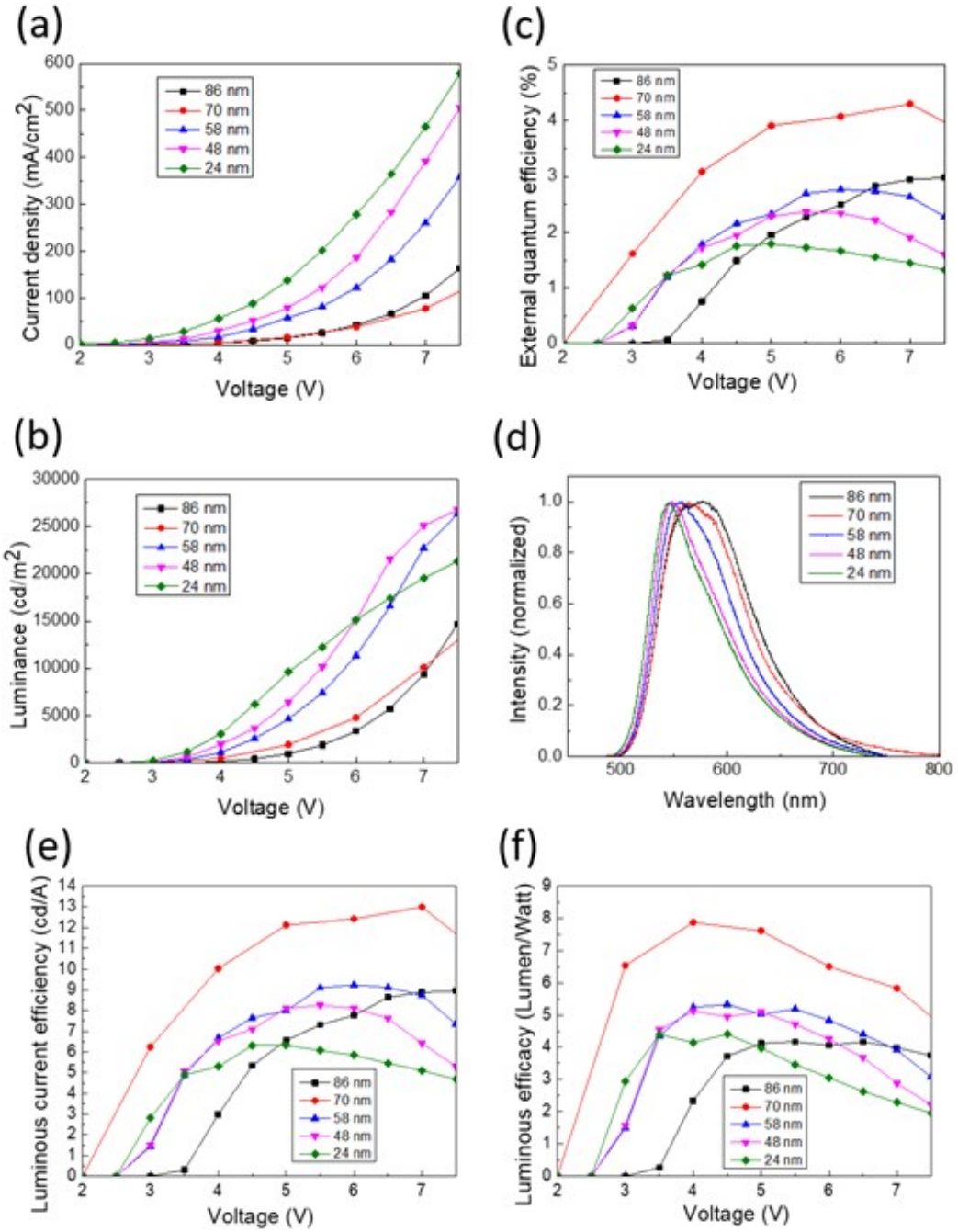

Figure S35: The electric performance of OLED device without chiral perovskites with various thickness of the emissive layer

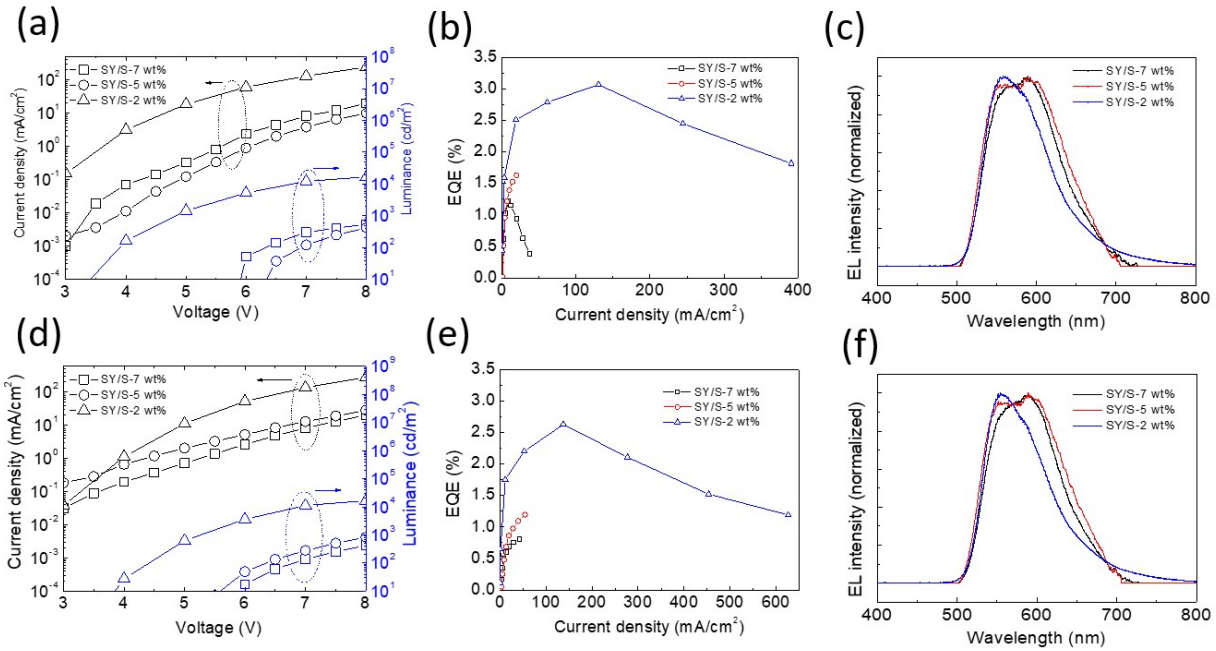

Figure S36: Performance of device based on (a,b,c) CB-treated and (d,e,f) untreated (S-BA)$_2$PbI$_4$,(a,d) J-V-L curves as a function of voltage (b,e) EQE as a function of current density and (c,f) normalized EL as a function of wavelength.

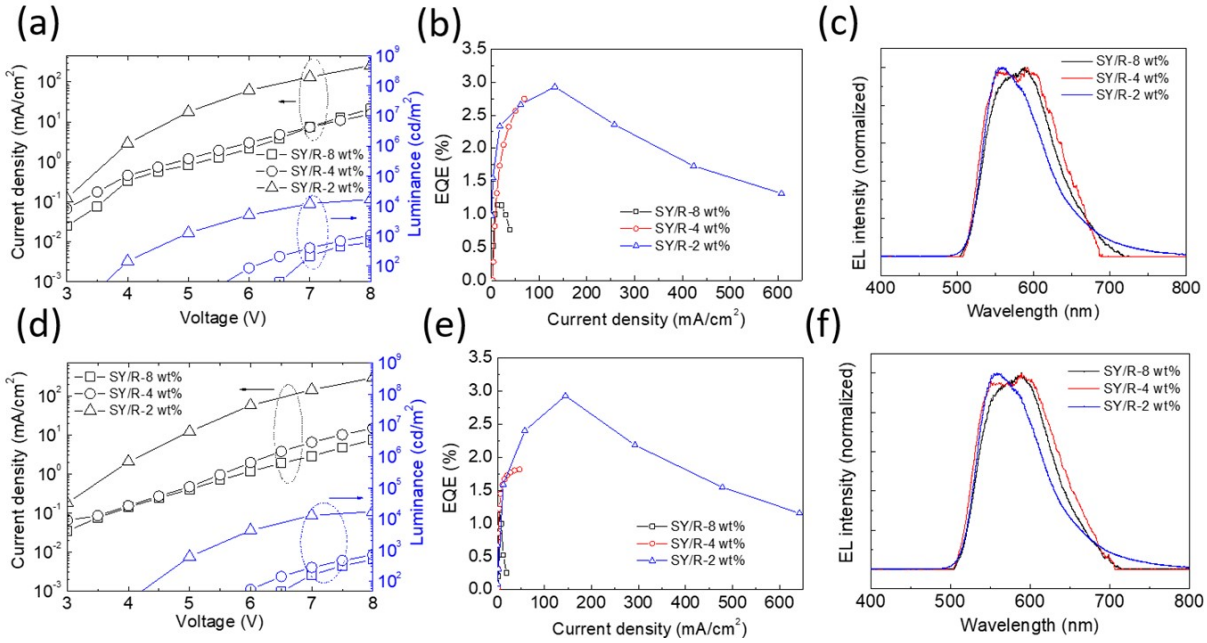

Figure S37: Performance of device based on (a,b,c) CB-treated and (d,e,f) untreated (R-BA)$_2$PbBr$_4$,(a,d) J-V-L curves as a function of voltage (b,e) EQE as a function of current density and (c,f) normalized EL as a function of wavelength.

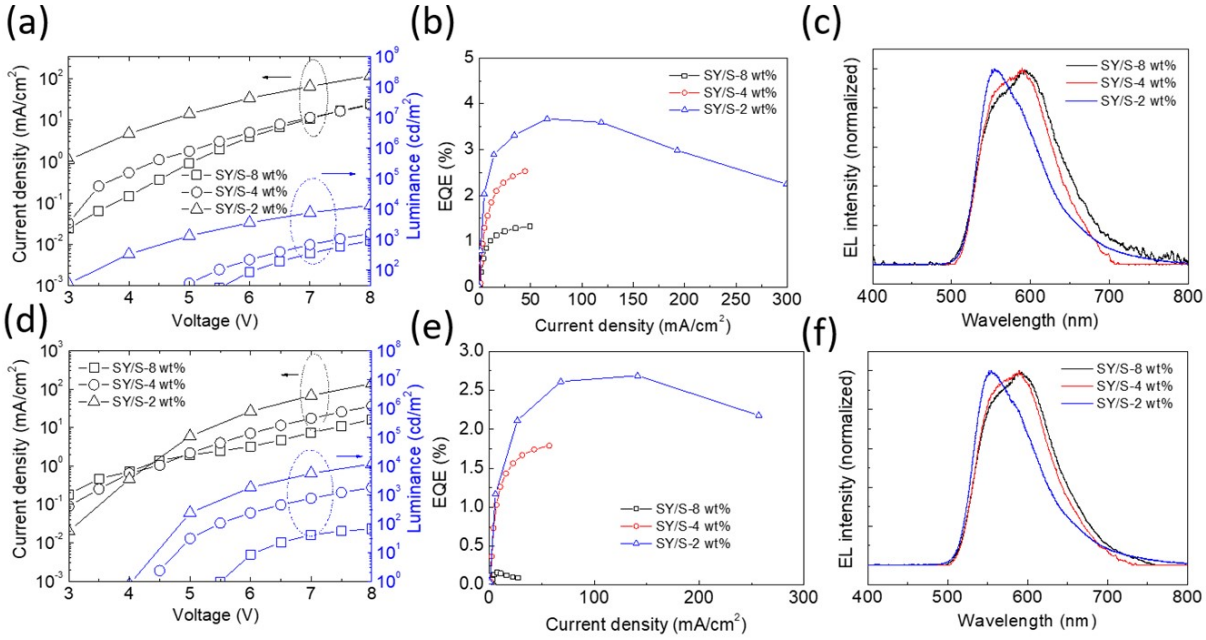

Figure S38: Performance of device based on (a,b,c) CB-treated and (d,e,f) untreated (S-BA)$_2$PbBr$_4$,(a,d) J-V-L curves as a function of voltage (b,e) EQE as a function of current density and (c,f) normalized EL as a function of wavelength.

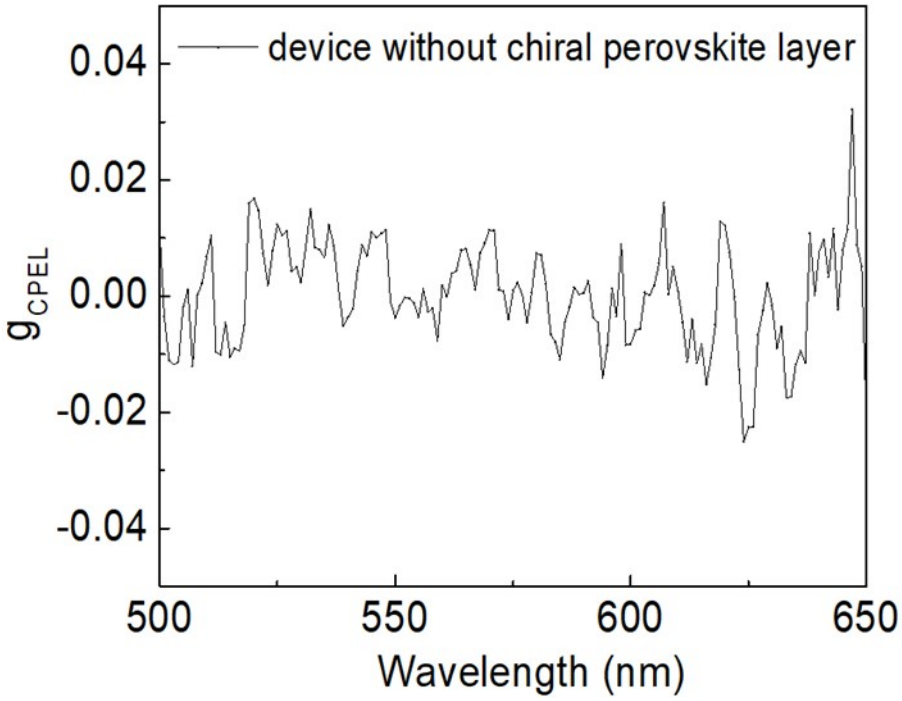

Figure S39: The g_{CPEL} as a function of wavelength for OLED device without chiral perovskites as CISS layer

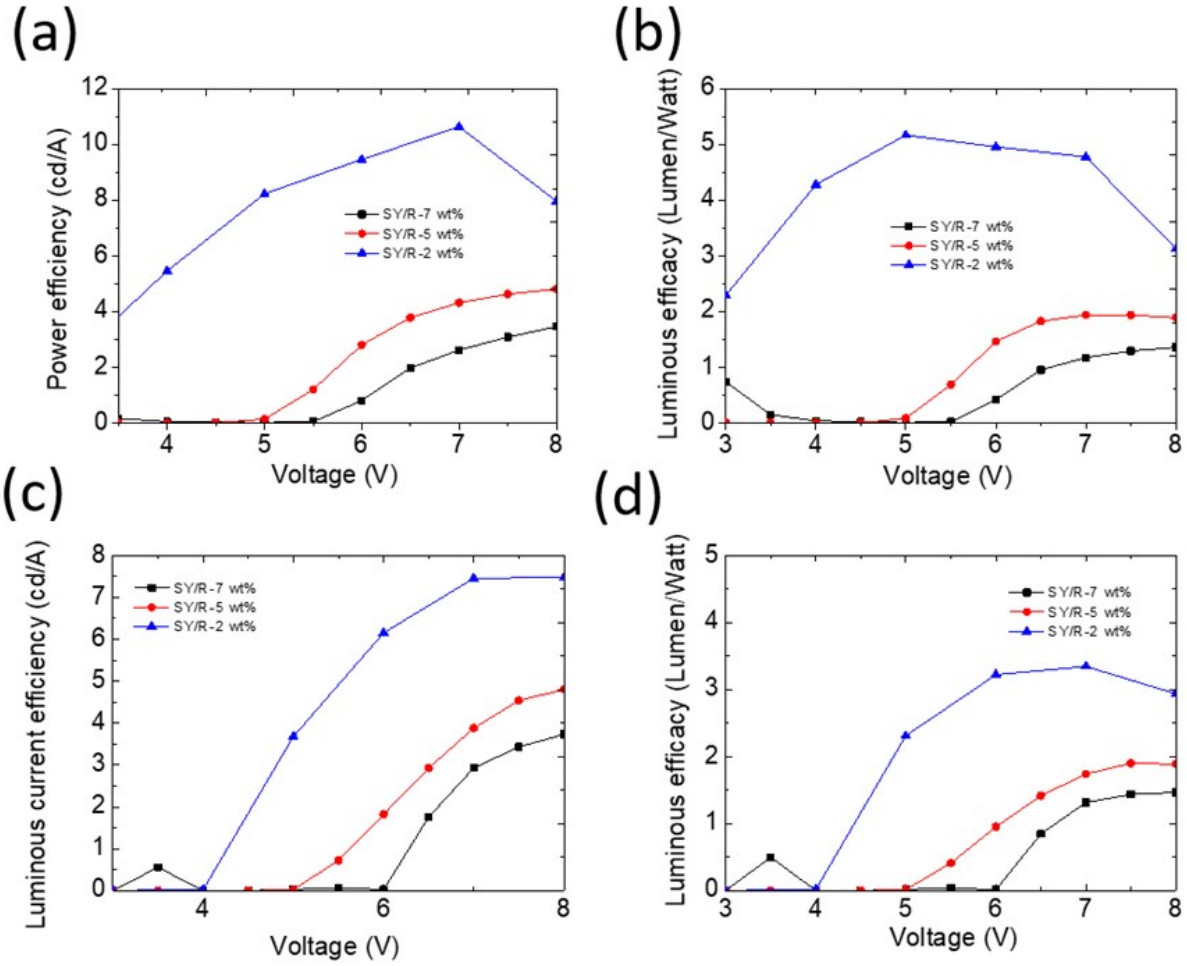

Figure S40: Performance of device based on (a,b) CB-treated and (c,d) untreated (R-BA)$_2$PbI$_4$,(a,c) power efficacies (Cd/A) and (b,d) luminous efficacies (Lm/W) as a function of voltage

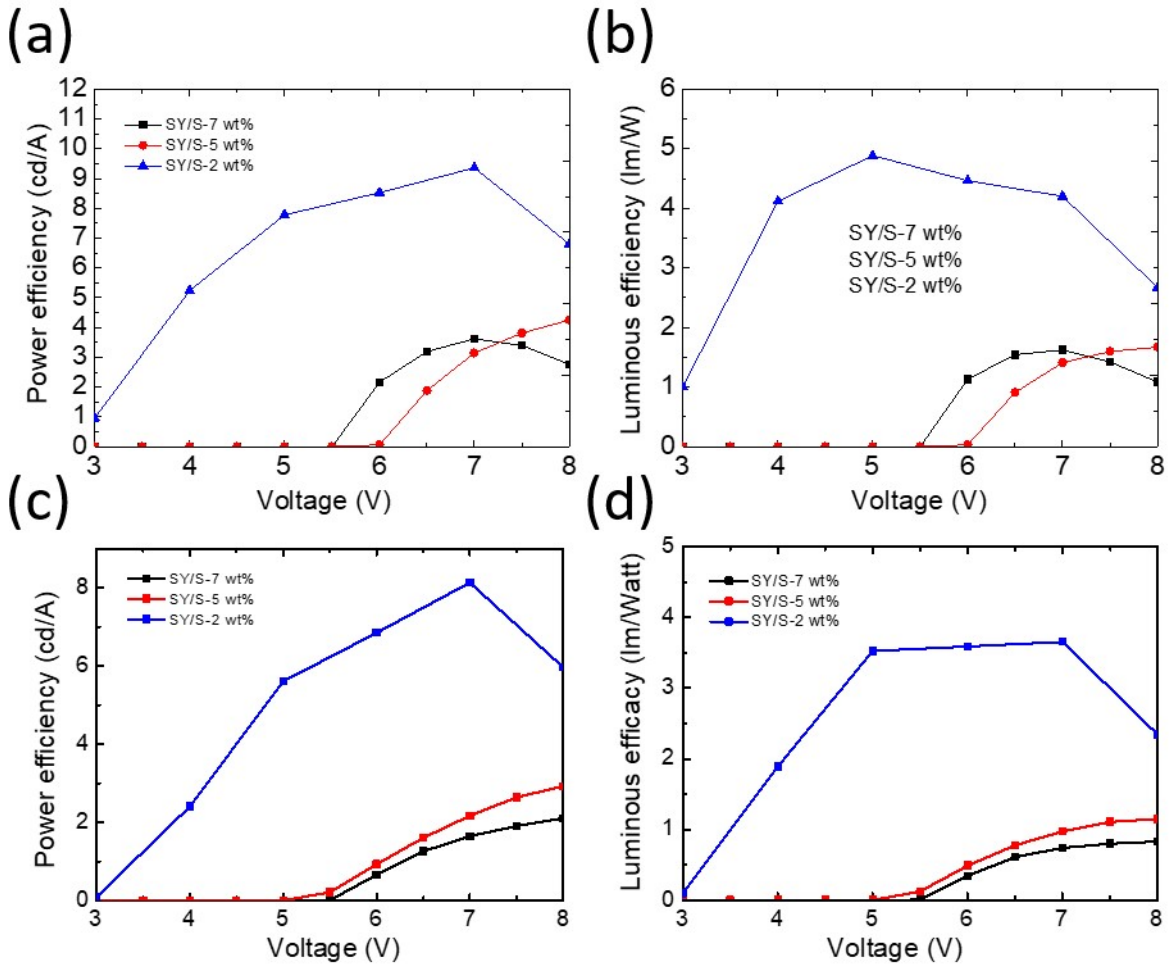

Figure S41: Performance of device based on (a,b) CB-treated and (c,d) untreated (S-BA)$_2$PbI$_4$,(a,c) power efficacies (Cd/A) and (b,d) luminous efficacies (Lm/W) as a function of voltage

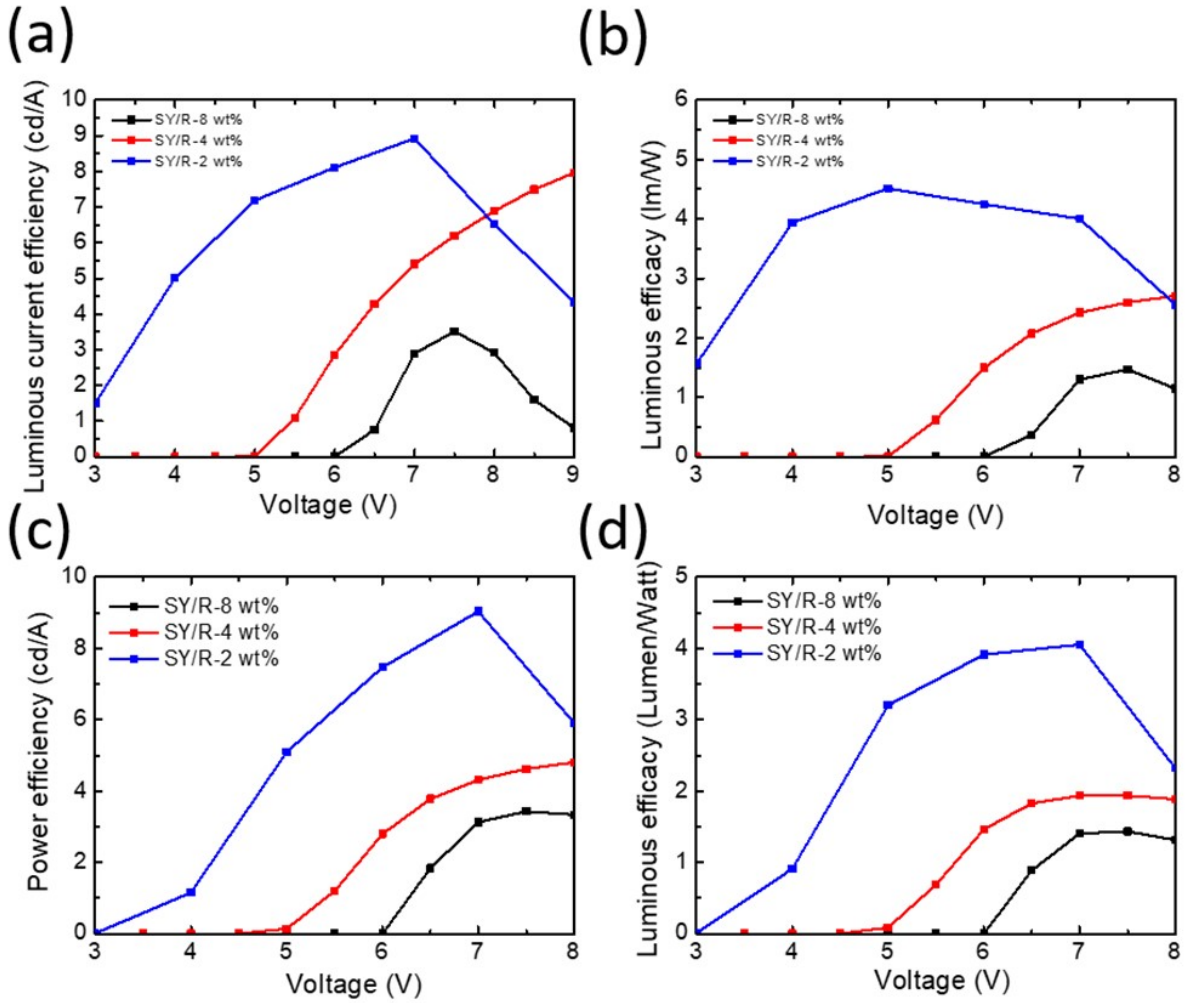

Figure S42: Performance of device based on (a,b) CB-treated and (c,d) untreated (R-$BA)_2PbBr_4$,(a,c) power efficacies (Cd/A) and (b,d) luminous efficacies (Lm/W) as a function of voltage

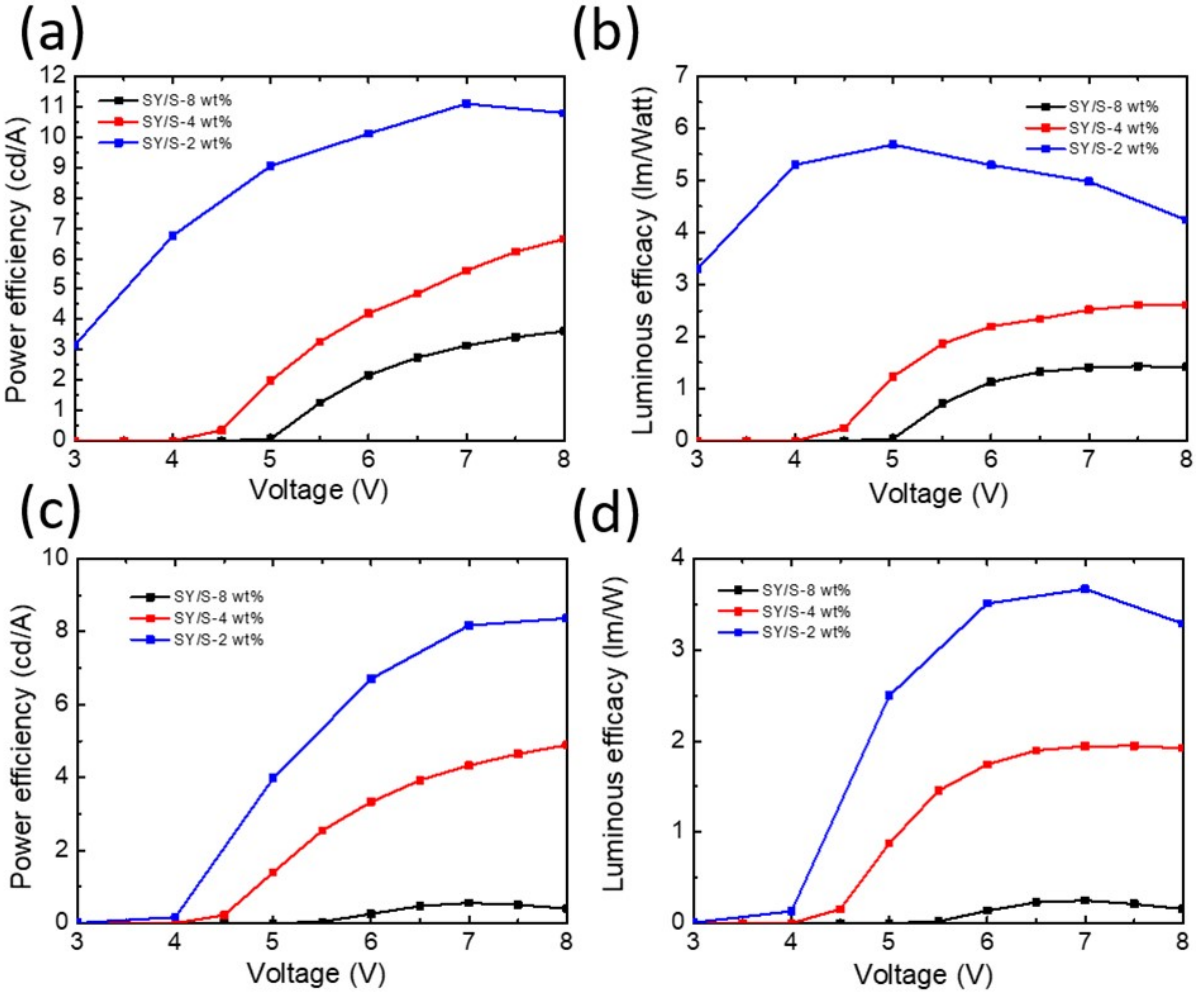

Figure S43: Performance of device based on (a,b) CB-treated and (c,d) untreated (S-BA)$_2$PbBr$_{4,}$(a,c) power efficacies (Cd/A) and (b,d) luminous efficacies (Lm/W) as a function of voltage

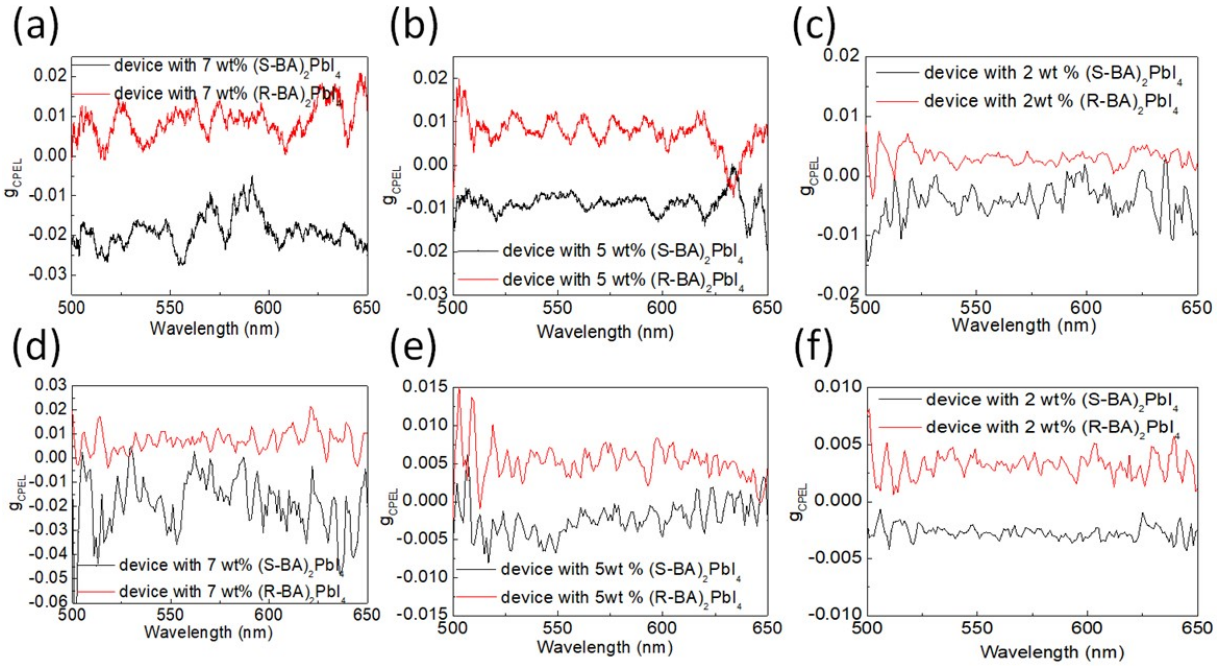

Figure S44: The $g_{CP\text{-}EL}$ of various precursor concentration as a function of wavelength, (a), (b)and (c) for the OLED devices based on (S-/R-BA)$_2$PbI$_4$ films with CB treatment and (d), (e)and (f) for the OLED devices based on (S-/R-BA)$_2$PbI$_4$ films without CB treatment.

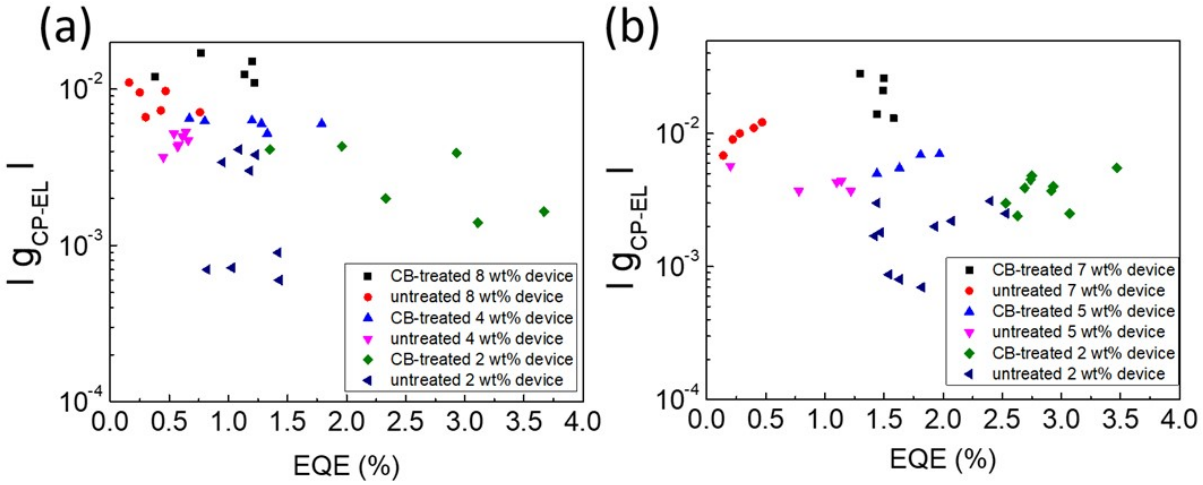

Figure S45: The statistics for $|g_{CP-EL}|$ and EQE of various chiral perovskites precursor concentration for spin-OLED devices based on CB-treated and untreated (a) $(S-/R-BA)_2PbBr_4$ films and (b) $(S-/R-BA)_2PbI_4$ films.

Table S1: The grain size and roughness of the CB-treated and untreated $(S\text{-}BA)_2PbBr_4$ films for different concentration of chiral perovskite

$(S\text{-}BA)_2PbBr_4$ film with CB treatment	**Film type**	**Size or roughness**	**$(S\text{-}BA)_2PbBr_4$ film without CB treatment**	**Film type**	**Size or roughness**
80 wt%	Smooth film	RMS=14.7nm	80 wt%	rough film	RMS=73.5nm
64wt%	Smooth film	RMS=11.5nm	64wt%	nanosheets	7um x 7um x 425nm
48 wt%	Smooth film	RMS=10.7nm	48 wt%	nanosheets	7um x 7um x 350nm
32 wt%	Smooth film	RMS= 8.56 nm/ (141.7 nm)	32 wt%	nanosheets	4um x 4um x 275nm
24 wt%	Smooth film	RMS= 7.56 nm/ (98.6 nm)	24 wt%	nanosheets	4um x 4um x 225nm
16 wt%	nanosheets	1um x 1um x 70nm	16 wt%	nanosheets	3um x 3um x 140nm
12 wt%	nanosheets	1um x 1um x 40nm	12 wt%	nanosheets	2um x 2um x 90nm
8 wt%	nanosheets	1um x 1um x 30nm	8 wt%	nanosheets	1um x 1um x 70nm
4 wt%	nanosheets	0.9um x 0.9um x 30nm	4 wt%	nanosheets	0.8um x 0.8um x 30nm
2 wt%	nanosheets	0.8um x 0.8um x 30nm	2 wt%	nanosheets	0.5um x 0.5um x 30nm

Table S2:The gabs of the CB-treated and untreated $(S\text{-}BA)_2PbBr_4$ films for different concentration of chiral perovskite in the presence of a magnetic field

$(S\text{-}BA)_2PbBr_4$ film with CB treatment	**g_{MCD} under +1.6T/-1.6T**	**$(S\text{-}BA)_2PbBr_4$ film without CB treatment**	**g_{MCD} under +1.6T/-1.6T**
80 wt%	-0.0042/0.0038	80 wt%	-0.0016/0.0007
64 wt%	-0.0041/0.0034	64 wt%	-0.0019/0.0018
48 wt%	-0.0031/0.0028	48 wt%	-0.0029/0.0029
32 wt%	-0.0043/0.004	32 wt%	-0.0018/0.0018
24 wt%	-0.005/0.0047	24 wt%	-0.0023/0.0024
16 wt%	-0.0057/0.0052	16 wt%	-0.0029/0.003
12 wt%	-0.0034/0.0034	12 wt%	-0.0023/0.0022
8 wt%	-0.0021/0.002	8 wt%	-0.0019/0.0019
4 wt%	-0.001/0.0011	4 wt%	-0.0016/0.0017
2 wt%	-0.0013/0.0014	2 wt%	-0.0011/0.0011

Table S3: The gabs of the CB-treated and untreated $(S\text{-}BA)_2PbI_4$films for different concentration of chiral perovskite in the presence of a magnetic field

$(S\text{-}BA)_2PbI_4$ film with CB treatment	**g_{MCD} under +1.6T/-1.6T**	**$(S\text{-}BA)_2PbI_4$ film without CB treatment**	**g_{MCD} under +1.6T/-1.6T**
80 wt%	-0.0002/0.0022	80 wt%	-0.00156/0.00151
60 wt%	-0.0029/0.0028	60 wt%	-0.00159/0.00173
30 wt%	-0.0032/0.0029	30 wt%	-0.00157/0.0016
25 wt%	-0.0015/0.0016	25 wt%	-0.00108/0.00122
20 wt%	-0.0015/0.0015	20 wt%	-0.00089/0.00105
15 wt%	-0.0011/0.0013	15 wt%	-0.00115/0.0013
10 wt%	-0.0014/0.0011	10 wt%	-0.0009/0.00117
7 wt%	-0.0014/0.0015	7 wt%	-0.0011/0.0011
5 wt%	-0.001/0.0013	5 wt%	-0.001/0.0012
2 wt%	-0.0011/0.0011	2 wt%	-0.001/0.0012

Table S4: The g_{MCD} of the CB-treated and untreated $(R\text{-}BA)_2PbBr_4$films for different concentration of chiral perovskite in the presence of a magnetic field

$(R\text{-}BA)_2PbBr_4$ film with CB treatment	**g_{MCD} under +1.6T/-1.6T**	**$(R\text{-}BA)_2PbBr_4$ film without CB treatment**	**g_{MCD} under +1.6T/-1.6T**
80 wt%	-0.0031/0.0034	80 wt%	-0.0007/0.0019
64 wt%	-0.0021/0.0026	64 wt%	-0.0023/0.0023
48 wt%	-0.0027/0.0035	48 wt%	-0.0028/0.0025
32 wt%	-0.0034/0.0038	32 wt%	-0.0017/0.0018
24 wt%	-0.0039/0.0039	24 wt%	-0.002/0.002
16 wt%	-0.005/0.0049	16 wt%	-0.0023/0.0023
12 wt%	-0.0025/0.0025	12 wt%	-0.0026/0.0026
8 wt%	-0.0023/0.0022	8 wt%	-0.0019/0.0019
4 wt%	-0.0022/0.0021	4 wt%	-0.0015/0.0014
2 wt%	-0.0005/0.0006	2 wt%	-0.0002/0.0006

Table S5: The g_{MCD} of the CB-treated and untreated $(R\text{-}BA)_2PbI_4$films for different concentration of chiral perovskite in the presence of a magnetic field

$(R\text{-}BA)_2PbI_4$ film with CB treatment	**g_{MCD} under +1.6T/-1.6T**	**$(R\text{-}BA)_2PbI_4$ film without CB treatment**	**g_{MCD} under +1.6T/-1.6T**
80 wt%	-0.0008/0.0008	80 wt%	-0.0016/0.0015
60 wt%	-0.003/0.0032	60 wt%	-0.0014/0.0015
30 wt%	-0.0008/0.0013	30 wt%	-0.0013/0.0014
25 wt%	-0.0015/0.002	25 wt%	-0.0015/0.0015
20 wt%	-0.0013/0.0014	20 wt%	-0.0015/0.0017
15 wt%	-0.0008/0.0012	15 wt%	-0.0011/0.0013
10 wt%	-0.0007/0.0012	10 wt%	-0.00082/0.0011
7 wt%	-0.0009/0.0011	7 wt%	-0.00088/0.001
5 wt%	-0.001/0.0013	5 wt%	-0.00087/0.0013
2 wt%	-0.0011/0.0012	2 wt%	-0.0005/0.0007

Table S6: The Rashba splitting and Zeeman splitting of the CB-treated and untreated (S-$BA)_2PbBr_4$ films for different concentration of chiral perovskite

(S-BA)$_2$PbBr$_4$ film with CB treatment	**Rashba splitting ΔE under 0 Tesla**	**Zeeman splitting ΔE under +-1.6 Tesla**	**(S-BA)$_2$PbBr$_4$ film without CB treatment**	**Rashba splitting ΔE under 0 Tesla**	**Zeeman splitting ΔE under +1.6 Tesla**
32 wt%	29.9 μeV	+-315 μeV	32 wt%	~10 μeV	+-286 μeV
24 wt%	20.3 μeV	+-240 μeV	24 wt%	~10 μeV	+-370 μeV
16 wt%	12.4 μeV	+-380.3μeV	16 wt%	~10 μeV	+-372 μeV
12 wt%	~10 μeV	+-376μeV	12 wt%	~10 μeV	+-355 μeV
8 wt%	~10 μeV	+-334 μeV	8 wt%	~10 μeV	+-339 μeV

Table S7: Summary on EL parameters of spin OLED device based on CB-treated and untreated (S-/R-BA)$_2$PbI$_4$ films as CISS layer

	Luminance$_{max}$ [cd m^{-2}]	**EQE$_{max}$ [%]**	**Power efficiency [Cd/A]**	**luminous efficiency [lm/W]**
CB-treated R form-7wt% devices	336	1.51	3.46	1.36
CB-treated R form-5wt% devices	715	1.82	4.8	1.94
CB-treated R form - 2wt% devices	16803	3.47	10.63	5.17
untreated R form - 7wt% devices	208	1.49	3.73	1.47
untreated R form - 5wt% devices	639	1.82	4.8	1.9
untreated R form - 2wt% devices	11520	2.4	7.48	3.35
CB-treated S form - 7wt% devices	438	1.22	3.62	1.62
CB-treated S form - 5wt% devices	938	1.63	4.3	1.67
CB-treated S form - 2wt% devices	18063	3.07	9.4	4.89
untreated S form - 7wt% devices	772	0.69	2.11	0.83
untreated S form - 5wt% devices	1889	1.2	2.92	1.15
untreated S form - 2wt% devices	18722	2.63	8.14	3.65

Table S8: Summary on EL parameters of spin OLED device based on CB-treated and untreated (S-/R-BA)$_2$PbBr$_4$ films as CISS layer

	Luminance$_{max}$ [cd m^{-2}]	**EQE$_{max}$ [%]**	**Power efficiency [Cd/A]**	**luminous efficiency [lm/W]**
CB-treated R form - 8wt% devices	309	1.14	3.5	1.47
CB-treated R form - 4wt% devices	2339	2.75	6.89	2.71
CB-treated R form - 2wt% devices	19098	2.94	8.92	4.52
untreated R form - 8wt% devices	772	1.2	3.43	1.43
untreated R form - 4wt% devices	2416	1.82	4.81	1.94
untreated R form - 2wt% devices	18746	2.93	9.03	4.05
CB-treated S form - 8wt% devices	1900	1.33	3.61	1.43
CB-treated S form - 4wt% devices	3223	2.53	6.65	2.61
CB-treated S form - 2wt% devices	17563	3.68	11.1	5.69
untreated S form - 8wt% devices	79	0.163	0.55	0.25
untreated S form - 4wt% devices	3578	1.791	4.89	1.94
untreated S form - 2wt% devices	16201	2.69	8.37	3.67

Table S9**:** Relevant chiroptical properties reported for the chiral perovskite applied to spin-LEDs.

Spin filter	Emissive layer	**EQE [%](max)**	**luminous efficiency max[lm/W]**	**Power efficiency [cd/A](max)**	**Luminescence dissymmetry factor gCPEL(max)**	**Ref.**
CB-treated **(R-BA)$_2$PbI$_4$**-7wt%	Organic polymer	1.51	5.17	3.46	0.016	This work
CB-treated **(S-BA)$_2$PbI$_4$** - 7wt%	Organic polymer	1.22	1.62	3.62	-0.026	This work
CB-treated **(R-BA)$_2$PbI$_4$** - 2wt%	Organic polymer	3.47	1.36	10.63	0.0055	This work
CB-treated **(S-BA)$_2$PbI$_4$** - 2wt%	Organic polymer	3.07	4.89	9.4	-0.0048	This work
CB-treated **(R-BA)$_2$PbBr$_4$** - 8wt%	Organic polymer	1.14	1.47	3.5	0.015	This work
CB-treated **(S-BA)$_2$PbBr$_4$** - 8wt%	Organic polymer	1.33	1.43	3.61	-0.017	This work
CB-treated **(R-BA)$_2$PbBr$_4$** - 2wt%	Organic polymer	2.94	4.52	8.92	0.0041	This work
CB-treated **(S-BA)$_2$PbBr$_4$** - 2wt%	Organic polymer	3.68	5.69	11.1	-0.0039	This work
(R-MBA)$_2$PbI$_4$	QDs (CdSe)	0.9	-	-	0.02	[24]
(S-MBA)$_2$PbI$_4$	QDs (CdSe)	1	-	-	-0.005	[24]
-	$MAPbBr_3$ NCs with with a chiral low-dimensional perovskite shell	-	-	-	+-0.006	[95]
-	Quasi-2D chiral perovskites	3.7	-	-	+0.004	[96]
-	Quasi-2D chiral perovskites	3.7	-	-	-0.0032	[96]
(R-MBA)$_2$PbI$_4$	$CsPbI_3/Br_3$ NCs	10	-	-	+0.026	[19]
(S-MBA)$_2$PbI$_4$	$CsPbI_3/Br_3$ NCs	10.5	-	-	-0.026	[19]